UNIVERSIDADE FEDERAL DO RIO GRANDE DO SUL

ESCOLA DE ENGENHARIA

PROGRAMA DE PÓS-GRADUAÇÃO EM ENGENHARIA ELÉTRICA

DIOGO TORRES CARDOSO

STUDY ON THE EFFICIENCY OF UHF RFID TECHNOLOGY FOR PASSENGERS' REGOGNITION IN INTELLIGENT PUBLIC TRANSPORTATION SYSTEMS

Porto Alegre

2019

DIOGO TORRES CARDOSO

STUDY ON THE EFFICIENCY OF UHF RFID TECHNOLOGY FOR PASSENGERS' RECOGNITION IN INTELLIGENT PUBLIC TRANSPORTATION SYSTEMS

Thesis presented to the Programa de Pós-Graduação em Engenharia Elétrica (PPGEE) of Universidade Federal do Rio Grande do Sul as part of requirements to obtain the title of Master in Electrical Engineering.

Area: Control and Automation

ADVISOR: Prof. Dr. Edison Pignaton de Freitas

Porto Alegre

2019

DIOGO TORRES CARDOSO

STUDY ON THE EFFICIENCY OF UHF RFID TECHNOLOGY FOR PASSENGERS' RECOGNITION IN INTELLIGENT PUBLIC TRANSPORTATION SYSTEMS

This thesis was judged adequate to obtain the title of Master in Electrical Engineering and was approved in its final form by the Advisor and Examination Board.

Advisor: _____

Prof. Dr. Edison Pignaton de Freitas, UFRGS

Doctor by Universidade Federal do Rio Grande do Sul – Porto Alegre, Brazil and Högskolan i Halmstad – Halmstad, Sweden

Examination Board:

Prof. Dr. Juliano Araujo Wickboldt, UFRGS

Doctor by Universidade Federal do Rio Grande do Sul – Porto Alegre, Brazil

Prof. Dr. João Cesar Netto, UFRGS

Doctor by Université Catholique de Louvain – Leuven, Belgium

Prof. Dr. Ivan Müller, UFRGS

Doctor by Universidade Federal do Rio Grande do Sul – Porto Alegre, Brazil

PPGEE coordinator: _____

Prof. Dr. João Manoel Gomes da Silva Jr.

Porto Alegre, June, 2019.

ESTUDO SOBRE A EFICIÊNCIA DA TECNOLOGIA RFID UHF PARA O RECONHECIMENTO DE PASSAGEIROS EM SISTEMAS DE TRANSPORTES PÚBLICOS INTELIGENTES

A locomoção coletiva de indivíduos no ambiente urbano é chamada de transporte público e pode ser representada de diversas formas. Em países em desenvolvimento, incluindo o Brasil, o transporte público é formado basicamente por um sistema rodoviário composto por ônibus de vários modelos e tamanhos, os quais dividem as vias públicas com carros, motos e outros, gerando um colapso viário, pois a maioria das cidades não foram preparadas para tal diversidade e volume de veículos. Uma forma de diminuir a quantidade de veículos nas ruas é melhorando os serviços públicos de tal forma que outros meios de locomoção sejam deixados de lado em prol de transportes públicos eficientes. O conceito de cidades inteligentes, muito debatido nos dias atuais, foca na tecnologia como a aliada no combate aos problemas existentes em diversas áreas, incluindo a locomoção dos indivíduos (HILDÉN, 2016).

Atualmente pesquisas apontam que o transporte público já enfrenta diversos problemas e insatisfações, os quais só tenderiam a aumentar se mais usuários passassem a usufruir do serviço disponibilizado. Por isso é necessário investir em tecnologias que auxiliem na melhoria do transporte público. Ter uma frota de ônibus que opera em horários determinados, sem atrasos, com veículos adequados para o volume de passageiros que venham a fazer uso do serviço, é o que a população espera (ALBUQUERQUE, 2014).

A proposta deste trabalho visa colaborar com este anseio da população apresentando uma solução para um problema vinculado às possibilidades futuras de soluções macros, o reconhecimento de passageiros. Quando aplicado com um sistema de geo-posicionamento, ele permite o reconhecimento das origens e destinos dos passageiros, de modo que as demandas e períodos específicos do dia possam ser avaliadas para um planejamento eficaz do sistema. Este trabalho apresenta um estudo sobre um sistema de reconhecimento de passageiros para o transporte público através do uso da tecnologia RFID UHF. Ele parte da proposta dos usuários continuarem utilizando seus cartões de validação, mas estes teriam uma etiqueta RFID UHF de forma que o passageiro não precise expor o cartão a algum equipamento e sim só portem ele em alguma parte do corpo, seja no bolso, carteira, mochila e etc.

Conforme destacado por (MALISON, 2008), o corpo humano é composto principalmente de água, o que afeta diretamente a leitura de etiquetas RFID, por isso neste trabalho é apresentado o estudo de uma etiqueta protótipo que se adeque melhor nesta aplicação.

Utilizando um sistema leitor (antenas e módulo) de mercado, são avaliadas etiquetas comerciais e o protótipo desenvolvido para certificação de performance e eficiência do sistema proposto. Testes preliminares com dois usuários de diferentes biotipos auxiliam na definição da melhor estrutura de leitura e na avaliação das diferentes etiquetas. Em seguida, com a estrutura de leitura definida e com a etiqueta de melhor performance selecionada, testes coletivos com um grupo de 10 usuários são realizados para avaliação da repetibilidade e da eficácia do sistema de reconhecimento. Ensaios finais em laboratório especializado, são realizados para avaliar as características da etiqueta desenvolvida para a aplicação.

Os resultados adquiridos fornecem uma base para avaliação da adequação e aplicabilidade do sistema idealizado e também dão abertura para futuros trabalhos de aperfeiçoamento da técnica utilizada.

Palavras chave: Reconhecimento de passageiros. Sistema de transporte público. Tecnologia RFID UHF. Etiqueta

ACKNOWLEDGMENTS

ABSTRACT

The automatic recognition of passengers in public transport systems has been a crucial point in mobility systems towards enhancements in passengers' flow and overall system efficiency. It allows the recognition of passengers' origins and destinations, so that the specific demands for specific periods of the day can be assessed for an effective system planning. However, this automatic control has to be efficient and smooth so that it does not incur in additional overhead to the entire system. This work presents a study on a passenger recognition system for public transport through the use of UHF RFID technology using EPC Gen2 standard. Preliminary tests were performed with two different forms of voluntary order to evaluate different types of tags. These tests first evaluated the height and angle of the antennas using 1, 2, 3 and 4 antennas in the tag recognition. From the results of these first tests, a set up was defined and then applied to a second evaluation now with 10 volunteers, which evaluated repeatability and effectiveness of the system for recognition. Moreover, additional laboratory-based tests were performed to access the effectiveness of the proposed recognition system. The acquired results provide a basis for evaluation the suitability and applicability of the proposed system.

Keywords: Recognition of Passengers. Public Transport Systems. UHF RFID Technology. Tag

SUMMARY

ILLUSTRATION LIST

TABLE LIST

ABBREVIATION LIST

AFC: Automatic Fare Collection

ANATEL: Brazilian National Telecommunications Agency

ANOVA: Analysis of Variance

ASK: Amplitude Shift Keying

BMI: Body Mass Index

CPqD: Center for Research and Development in Telecommunications

CRC: Cyclic Redundancy Check

EAN: European Article Numbering Association

EAS: Electronic Article Surveillance

EEPROM: Electrically Erasable Programmable Read-Only Memory

EPC: Electronic Product Code

FSK: Frequency Shift Keying

GSM: Global System for Mobile Communications

GS1: Global System 1

HF: High Frequency

IC: Integrated Circuit

ID: Identification

ISO: International Organization for Standardization

LED: Light Emitting Diode

LF: Low Frequency

LHCP: Left Hand Circular Polarization

MAC: Media Access Control

MF: Microwave Frequency

MIT: Massachusetts Institute of Technology

M6e: ThinkMagic Mercury6e

PET: Polyethylene Terephthalate

PSK: Phase Shift Keying

RF: Radio Frequency

RFID: Radio Frequency Identification

RHCP: Right Hand Circular Polarization

RJ: Ryan-Joiner Model

ROM: Read Only Memory

RSSI: Received Signal Strength Indication

SAW: Surface Acoustic Wave

UHF: Ultra-High Frequency

UCC: Uniform Code Council

1 INTRODUCTION

Public transport is defined as the form of collective locomotion in the urban environment of individuals from different socioeconomic backgrounds (HILDÉN, 2016). In developing countries, including Brazil, the high costs of investing in the infrastructure of subway lines end up leading public transport to basically be formed by a road system consisting of buses of various models and sizes. The bus fleet of most Brazilian metropolises divides public streets with cars, motorcycles and others, forcing the cities to be prepared for such diversity and volume of vehicles. An infrastructure failure can end up generating a road collapse, resulting in congestion, delays and different types of inconvenience for its users (BRAGA, 2016).

Research in recent years shows that public transportation in Brazil lacks effective investments and the reflection of this is the lack of interest of the population to use the service. Only those who really depend on the bus are the ones who use it, and even so, research shows that the general satisfaction of the population does not reach 30% (ALBUQUERQUE, 2014). Factors such as vehicle quality, itinerary (route of traffic), time of travel, timetables and number of passengers, directly affect this service satisfaction index (HU, 2015). Environmental issues related to pollution, which should be an important factor in the choice of means of transport (BRAGA, 2016), end up being succumbed to the other factors already named.

Today in smart cities context, one of the most important factors is precisely intelligent transportation systems, which aim to bring convenience and comfort to public transport users. One way to achieve this goal is to facilitate operational management by companies providing public transport services (HILDÉN, 2016).

With the goal of addressing this scenario, municipal transit regulatory agencies and transport service providers have been introducing automatic vehicle monitoring systems. These systems are capable of performing fleet tracking, evaluating the operational performance of the

service and providing information about the transport network. Basically the system consists of a central node that receives data online from vehicles, including geo-positioning. These systems exploit static and dynamic data. Static data include general information about the public transport service, such as paths, stops, routes schedules, while the dynamic ones are the status of each vehicle, including number of users at any given time (FIORI, 2016).

The large amount of information obtained on a daily basis requires a specialized evaluation to result in improvements in the service. Following this section, several papers were published focusing on the analysis of the dynamic data obtained to learn how the population uses public transport and thereby improve the service provided (GAL, 2017; ZHANG, 2016). These studies assume that passenger counting is effective, but as reported (OBERLI, 2010) there are a number of factors that generate losses and therefore these numbers do not describe the actual scenario of use.

In this context, the present work focuses on this area that needs improvements and proposes a new way of recognizing the flow of urban transport passengers through UHF RFID technology. With the use of portable passive antennas, each user who owns a tag creates the possibility not only of actual passenger counting but also the recognition of which passenger is attached to the vehicle. This information combined with other data already controlled by the fleet management system enables the improvement of the service provided to the population.

The thesis is organized as follows. Chapter 2 reviews the theoretical basis of radio frequency identification and ultra-high frequency. Chapter 3 shows the technologies involved in the current market solutions and the new proposal, pointing out advantages and disadvantages. Chapter 4 describes the study methodology applied in this work. Chapter 5 summarizes the mathematical modeling to developing the passengers' tag. Chapter 6 presents the system deployment, detailing the readers' set and the prototype tag. Chapter 7 shows the

experimental setup and the results. Chapter 8 discusses the experimental results. Finally,

Chapter 8 concludes the work and suggests directions for future work.

2 THEORETICAL BASIS

In the following sections, important concepts will be described and necessary for the presentation of the study carried out in this work.

2.1 RADIO FREQUENCY IDENTIFICATION (RFID)

Radio Frequency Identification is a technology capable of capturing, managing, analyzing and responding to data from electronic sensors. RFID is an identification technology that uses radio frequency to capture data, allowing an RFID tag to be read without the need for contact or field of vision, through barriers and objects such as wood, plastic, paper, among others. It is a method of storing and retrieving data remotely. It works as a powerful real-time data acquisition system with the advantage of eliminating manual and visual human interventions, thus streamlining the transitions time and ensuring efficiency and effectiveness in the process (GLOVER, 2006).

The RFID system has four basic components: tag, transceiver, antenna, and middleware module. The operation of the RFID technology, as described in (GLOVER, 2006), involves a tag that transmits its identification code to the reader, it receives the code and makes it available to the application that will define what the system's functionality of RFID.

2.1.1 RFID System Components

The general architecture of an RFID system may vary according to the bibliography. (AHSON, 2008) consider it to have only two components: tag and reader. However, for didactic reasons and to facilitate the understanding of the RFID architecture, in this work it will be divided into four basic components: tag, antenna, reader and middleware module. RFID technology uses frequencies within the 30 kHz and 30 GHz range. In the following sections, the main components and classifications of the RFID system will be presented.

A. Tag

The tag, also called a transponder, identifier or RFID tag, is basically formed by a silicon microchip and an antenna, as shown in Figure 1.

Figure 1 - RFID tag
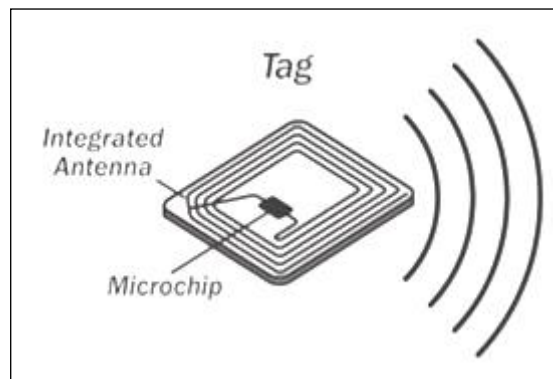
Source: TuffClassified.com website[1].

Usually, the tags are wrapped in plastic and can be encapsulated in several formats. Depending on the use of the tags, the choice of the format is fundamental, taking into account the durability, resistance to temperature changes and accessibility (GLOVER, 2006).

The purpose of a tag is to identify the living, object, or place to which it is attached because of its unique identification number (which may also be composed of strings): the Electronic Product Code (EPC).

There are several types of tags available on the market that meet the diverse needs of the applications. Therefore, tags can be classified by their different characteristics, such as: battery usage, encapsulation form, frequency, coupling and storage capacity.

- **Battery Usage**

The source of energy is the main factor of classification of the tags. According to (GREFF, 2009), they can be classified as passive, semi-passive and active.

---

[1] Available at: <https://tuffclassified.com/rfid-tag-manufacturing-company-in-india_1223996>. Access in: 7 Sep. 2018.

The passive tag usually contains Read Only Memory (ROM) and only responds to the signal from the antenna connected to the player. It operates without a battery, and its power is supplied by the reader itself through electromagnetic waves. This type of tag has a lower average range and theoretically infinite durability, since its useful life only has as limiting factor its good use (ROEHRIG, 2005).

By working at a lower frequency, these tags are more susceptible to noise and signal loss in relation to weather factors, barriers and/or transpositions. However, the cost of passive models is much lower, and has a much higher lifespan compared to active models.

The semi-passive tag is very similar to passive but incorporates a small battery that allows the integrated reading circuit to be constantly powered; and has a faster response time as it is more powerful in its reading range. This type of tag does not have an active transmitter, a fact that differentiates it from the active tags.

This type of tag is used in real-time systems for tracking high value materials or equipment within a factory. Another application of the semi-passive tag is in the temperature, pressure, relative humidity, acceleration, vibration, movement and altitude sensors in products that require this monitoring. It has better readability when attached to opaque and absorbent materials (GREFF, 2009).

The active tag is powered by an internal battery, which makes its life span limited. This type of tag has the characteristic of transmitting the signal itself, operating at high frequencies. This does not require the use of several antennas to cover a space, since its range is greater.

The main advantages of the active tag are: performing write and reading processes, increased memory capacity and noise tolerance and signal loss (AHSON, 2008). Its major drawbacks are high cost (in relation to passive tags), size and battery life.

- **Encapsulation Form**

The tags can be placed on buttons, plastic cards, paper labels, glass capsules, watches, bracelets, earrings, key chains, etc. They can be fixed on products or packaging, attached to pieces of clothing, placed on animals or even on people.

According to (HECKEL, 2007) depending on the use of the tags, the choice of format is fundamental, taking into account: durability, resistance, temperature changes and accessibility.

- **Frequency**

RFID tags can also be classified according to the frequency at which they operate. Frequency is a very important factor in adopting an RFID system because, according to it, there will be a greater or lesser range of range. Moreover, for (GLOVER, 2006) "different frequencies have different properties. Lower frequency signals are more capable of traveling through the water, while higher frequencies can carry more information. "Another factor in which frequency influence is the rate of data transfer: the higher the frequency, the higher the throughput of data.

The low frequency (LF) band includes frequencies between 30 kHz and 300 kHz. An advantage of this range is that it penetrates most materials, such as metals, water and the very skin of the human body. Its major disadvantage is the interference that can be caused by electric motors in industrial environments (AHSON, 2008). The frequency of 125 kHz is the most used in RFID systems, although there are also applications that use the frequency of 134 kHz.

LF tags have the lowest data throughput of all frequencies used in RFID and are generally used to store a small amount of data. The area of coverage of this signal can reach from a few centimeters up to 1.5 m, however, these tags are usually more expensive than the

others. Examples of application: identification of animals, identifiers attached to materials with high humidity or close to metals, access control, car control, vehicle immobilizers, etc.

According (AHSON, 2008), the high frequency (HF) band includes frequencies between 3 MHz and 30 MHz, with HF tags typically operating at 13.56 MHz. As an advantage over LF tags, these tags transmit data faster and can store a larger number of data. As a disadvantage, the HF range is more susceptible to interference when the tags are close to metals, and for this reason, their cost is lower. HF tags are usually passive, and have a reading range of up to 1.5 m. Examples of application: smart cards, credit cards, books, air baggage, libraries, electronic passports (e-passports), etc.

The ultra-high frequency (UHF) band includes frequencies between 300 MHz and 3 GHz, with only the 433 MHz and 860 MHz to 960 MHz frequencies being used for RFID applications (GLOVER, 2006). The first is used by active tags and the second by passive or semi-passive tags. This range is used when readers need to read tags at a greater distance than those obtained by the LF and HF bands. These tags can be easily coupled to various types of materials. Its manufacturing process is relatively simple, contributing to lower its cost. All protocols in the UHF range offer anti-collision capability, allowing multiple labels to be read simultaneously. Application examples: identification of boxes, special tracking of animals and logistics.

The microwave frequency (MF) band includes frequencies between 2 GHz and 30 GHz, with only the 2.45 GHz frequency being used in RFID applications. MF tags reach distances greater than the others and can be used by passive, semi-passive and active tags. Passive tags are less common in the market because they are more expensive than passive UHF tags and share the same advantages and disadvantages; the semi-passive are used to control long-range access for vehicles, fleet identification and toll collection on highways; and the active ones are used for real-time localization systems (GREFF, 2009).

- **Coupling**

The form of coupling is how the tags will communicate with the readers and can be fed by them in the case of passive tags. Each of the coupling forms uses a specific frequency and are recommended according to the distance between reader and tag.

Diffuse return coupling, also called a backscatter, is used in some active tags and in passive tags that need to be fed by the reader. Tags that use this type of coupling reflect the frequency of the player to generate power, which ranges from a few microwatts to a few milliwatts. As described (GLOVER, 2006), the chip in the tag controls a resistor that can reflect the signal of the reader in a smaller amplitude, so a modulated Amplitude Shift Keying (ASK) signal can be created to transmit the identifying number stored in the memory of the chip.

Inductive coupling is considered a remote coupling and is also used in passive tags that need the energy of the readers. The reading device generates an electromagnetic field at the frequencies of 135 KHz or 13.56 MHz which penetrates the coil area of the tag and induces a voltage that is retracted and used to power the chip, which will send its identification (ID) to the reading. Its operation occurs when the tag is in the reader's coverage area (interrogation zone) and its resonance frequency corresponds to the frequency of the reading device. Data modulation can be done by Amplitude Shift Keying (ASK), Frequency Shift Keying (FSK) or Phase Shift Keying (PSK). "The reading range of the tags that use this coupling mode is about 10 cm, and can be increased according to the size of the antennas used" (DOBKIN, 2013).

Figure 2 illustrates the inductive coupling of a tag and an antenna of a passive RFID system. The principle is similar to that of a transformer, where the antenna transfers energy and the data is exchanged between the two elements.

Figure 2 - Inductive coupling
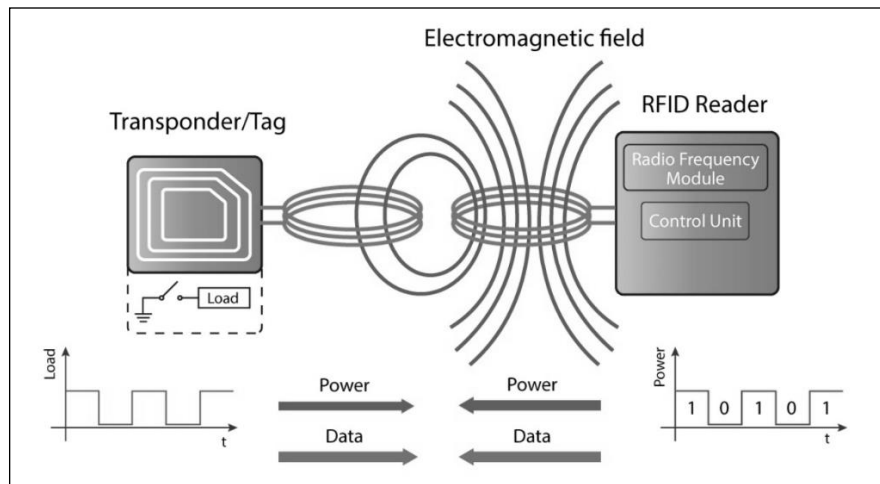
Source: DEVPOST website[1].

The magnetic coupling is very similar to the inductive, except that the antenna of the magnetic coupling reader is 'U' shaped. The distance between the player and the tag should not exceed 1cm. As explained (SANTINI, 2008), this type of coupling is based on the principle of electromagnetic proximity and requires that the area of the tag in 'magnetic contact' be maximum, (...) the electromagnetic flux should flow through the entire 'antenna' of the tag, otherwise the tag does not receive sufficient power to start operation. "

- **Storage Capacity**

Tags can also be classified for storage capacity. You should analyze each case to decide which is the best type of tag to use, because the higher the memory availability, the higher the cost. According to (HECKEL, 2007), the tags can have a bit up to a few bytes and can be classified in Electronic Article Surveillance (EAS), Surface Acoustic Wave (SAW) and N-bit Transponder.

EAS tags, also called '1-bit transponders', are passive and may have microchips (OLIVEIRA, 2006). They can only communicate if they are connected (via a value bit 1) or if they are switched off (bit equal to 0) (AHSON, 2008). It is the cheapest tag type and also the

---

[1] Available at: <https://devpost.com/software/rfidbls>. Access in: 21 Feb. 2018.

most used in the market. Its main application is in the control of objects and its common places of use are: libraries, movie rental stores and commercial stores.

SAW tags have a unique ID that has been recorded at the factory. These tags do not have batteries or microchips, they operate through microwaves and their ID cannot be modified.

For (GLOVER, 2006): "(...) the antenna receives the reader's microwave pulse and feeds it. The transducer has a piezo electric crystal that vibrates when it receives the microwave pulse. This vibration creates an acoustic wave that travels through the tag, finding reflector strips (on the right). The strips reflect the back of the wave, causing the crystal to vibrate again creating a return diffusion reflection. The number and spacing of the reflector strips determine the number and time of the pulses sent back to the reader, and also determines the number represented by the identifier. Practical restrictions on size also limit SAW identifiers to 32-bit capacity. (...) SAW identifiers represent a certain number that the reader 'illuminates' so that it becomes visible."

Figure 3 shows a SAW tag.

Figure 3 - SAW tag
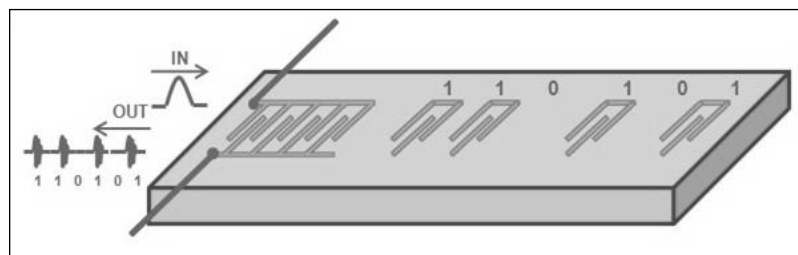
Source: JISIS website[1].

The n-bit transponder tags may have more information than a simple ID. To allow the use of additional information, you can use the Electrically-Erasable Programmable Read-Only Memory (EEPROM). These tags are more complex than the others, some of them use

---

[1] Available at: <http://www.av.it.pt/jisis/saw.html>. Access in: 21 Feb. 2018.

cryptography and anti-collision techniques when they are grouped with other tags. They can be passive or active (they are usually active), and may have complete microprocessors.

The EEPROM is responsible, in RFID applications, for storing the data in the tag. It must be non-volatile to ensure that the data is stored when the device is in its stand-by state. Its contents can be erased and rewritten several times electrically. (SANTINI, 2008).

B. Antenna

The antenna, also called a coil, performs communication within the RFID system. Its role is to define how the electromagnetic field will be generated, conformal performing the exchange of information between the reader and the tag (AHSON, 2008). The antenna emits a radio signal that activates the tag, reading or writing data, which after being read are sent to the middleware of the system. This radio wave emission is diffused in several directions and distances, depending on the power and frequency used. The elapsed time in this operation is less than one-tenth of a second, so the tag exposure time is very small. The antennas are offered in various shapes and sizes, according to the operational requirement of the application. Examples of antennas can be seen in Figure 4.

Figure 4 - RFID Antennas

Source: RFID4UStore website[1].

---

[1] Available at: <https://rfid4ustore.com/blog/how-to-select-an-rfid-antenna/>. Access in: 13 Dec. 2018.

Both the reader and the tags must have an antenna to be able to exchange information. However, the antenna can be considered as a separate element in the RFID systems, since in many applications, where more mobility is required, the antennas are coupled to the transceivers, being called readers (MORENO, 2016).

C. Reader

The reader, also called a transceiver, reader, or interrogator, is the communication component between the RFID system and external information processing systems. The complexity of the readers depends on the type of tag and the functions to be applied (AHSON, 2008). The most sophisticated players have error parity checking and data correction functions. Once the receiver signals are correctly received and decoded, algorithms can be applied to decide whether the signal is a response transmission of a tag.

Readers emit radio waves to feed the tags, which in turn return the requested information. (DOBKIN, 2013) explains that when the tag passes through the coverage area of the antenna, the magnetic field is detected by the reader, which decodes the data coded in the tag, passing them to the middleware to perform the processing. Data communication between tags and readers is performed without physical contact.

D. Middleware Module

The middleware module, also called an application or final software, is the interface device that controls the entire RFID peripheral system (reader and tags) in addition to communicating with the other components of the system. It is developed for integration between RFID applications and often goes unnoticed by running in the background in the system. The middleware is responsible for filtering the large number of data collected by the readers, for debugging the information received by the antennas, and for converting this information into something that the user's system can interpret.

For (GLOVER, 2006), there are three reasons to use RFID middleware: encapsulate the applications of the device interfaces; process the raw information captured by readers so that applications only see meaningful events; and for an application-level interface to manage readers and consult RFID system observations.

The development of middleware varies according to the hardware of each manufacturer and requires a high degree of technical knowledge, since most readers simply capture all the data that is in their interrogation area and it is up to the middleware to organize this data and transform it into information.

2.1.2 Patterns

The need for interoperability of RFID systems has led to the adoption of standards for working with radio frequency identifiers. The main existing identifiers follow the EPC or International Organization for Standardization (ISO) standards, and each of them works with different readers. For this reason, it is important to know these different standards and analyze the choice of the ideal reader depending on each application.

The purpose of standardization and standards is to define the platforms on which an industry can operate in an efficient and safe manner. The largest RFID manufacturers offer proprietary systems, resulting in a diversity of RFID system protocols in the same industrial plant (DOBKIN, 2013). As well-known organizations involved in the RFID standardization struggle, we can highlight the international EPC Global and ISO.

A. EPC Global

According to (DOBKIN, 2013) in the 1980s when Massachusetts Institute of Technology (MIT), together with other research centers, began to study an architecture that uses the resources of radiofrequency-based technologies to serve as reference model to the development of new product tracking and localization applications. From this study, the EPC

was born. The EPC defined a product identification architecture that utilized the resources provided by radio frequency signals, later called RFID.

In 2005, European Article Numbering Association (EAN), Uniform Code Council (UCC) and Global System 1 (GS1) formed the EPC Global, which according to (GLOVER, 2006) "defines a combined method of classifying identifiers that specifies frequencies, coupling, switching and modulation types, information storage capacity and modes of interoperability of RFID systems."

EPC Global defined an architecture for identification of products that used the radio frequency signals, which came to be called RFID. (HECKEL, 2007) states that: "An EPC establishes a unique number for a given product, similar to a Media Access Control (MAC) address of a network card."

The structure of the basic format of an EPC number can be analyzed in Figure 5.

Figure 5 - Structure of an EPC number
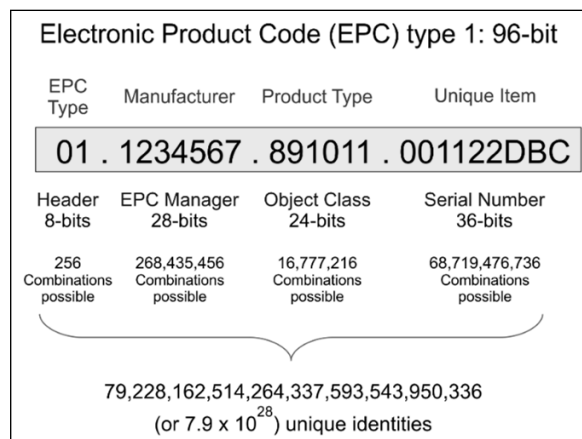
Source: End Times Truth website[1].

The header field indicates the length, type, structure, version, and generation of the EPC; the EPC manager number field is the entity responsible for maintaining the subsequent partitions; the object class identifies the class of the object to which the tag is attached; and the

---

[1] Available at: <https://endtimestruth.com/mark-of-the-beast/rfid/>. Access in: 7 Aug. 2017.

serial number identifies the instance. The different classes defined by EPC Global are listed in Table 1.

Table 1 - Class of tags recognized by EPC Global

Class	Description
0	Passive, read only
0+	Passive, write once, but using class 0 protocols
I	Passive, record once
II	Passive, record once with extras such as cryptography
III	Rewritable, semi-passive (chip with battery, communications with reader energy), integrated sensors
IV	Rewritable, active, identifiers can talk to other identifiers, energizing their own communications
V	They may energize and read Class I, II and III identifiers and read Class IV and V identifiers, as well as act as class IV identifiers

Source: Prepared by the author, 2019.

The schema of storing data in a tag can be seen in Figure 6.

Figure 6 - Storing data in a tag

Source: VERASSET page on SlideShare website[1].

The Cyclic Redundancy Check (CRC) field is a way to detect storage or transmission errors. It is sent with the original message and verified on the receiver in order to prove that

---

[1] Available at: <https://pt.slideshare.net/Verasset/verasset-rfid-overview?ref=>. Access in: 22 Oct. 2017.

there were no changes. The EPC field is the tag code and the password is the field responsible for disabling the tag, destroying it permanently.

B. ISO

As the first RFID systems were used only for internal control, there were no concerns regarding standardization for the technology. According to (DOBKIN, 2013), the first sector to request a standardization was the one of the cattle raising, for the application of identification of animals.

(GLOVER, 2006) explain that in February 2005, the EPC specification was submitted to ISO, and it is hoped that this will resolve some conflicts between the two approaches.

2.2 THE THEORY BEHIND THE UHF SOLUTION

The purpose of this chapter is to provide the necessary theoretical knowledge about RFID UHF. The main aspects and the mathematics behind the whole operation of technology.

2.2.1 UHF Wave Propagation

The knowledge of the physical properties of an UHF wave is vital to be able to design a tag antenna fitting the end application (DOBKIN, 2013).

A. Free Space Transmission

A free space transmission system consists typically of a transmitting antenna, a transmission path, and a receiving antenna (DOBKIN, 2013). Parameters of every component determine the functionality of the entire system.

The main criteria hereby are transmitted power, antenna parameters (gain, polarization and reflection coefficient), wavelength and distance between the transmitting and the receiving

antenna. The Friis Transmission Equation, Equation 1, describes the mathematical relation between these components:

$$P_R = P_T \left(\frac{\lambda}{4\pi R}\right)^2 G_T G_R \tag{1}$$

P_R: Transmitted Power

P_T: Received Power

R: Distance between transmitting and receiving antenna

λ: Wavelength

G_T: Gain of the transmitting antenna [dBi]

G_R: Gain of the receiving antenna [dBi]

G is measured relative to an isotropic antenna [dBi]

B. Absortion

Only vacuum is passed by electromagnetic energy without absorption. If an electromagnetic wave loses energy and this energy is converted into other forms, this process is called Damping or Attenuation (BALANIS, 2005).

The absorption is given by the imaginary part of the refractive index $\underline{n} = \sqrt{\varepsilon_r}$.

The absolute value of the field strength decreases along the propagation path.

The electrical field strength at a certain position x depends on two parameters: Distance (x) from the RF source and the properties of the media along the transmission path.

The propagation attenuation (or path loss) is calculated by referring to the ratio between the emitted electrical field strength at the source (antenna) and the electrical field strength at a certain distance x, after the transmission via the media. The propagation attenuation in dependency of the distance is given by equation 2.

$$A[dB] = 20\log\left|\frac{E(0)}{E(x)}\right| \tag{2}$$

The free space path loss at distance d is:

$$a_0[dB] = 20 \log \left| \frac{4\pi d}{\lambda} \right| \tag{3}$$

Many dielectric materials, like dry paper or cardboard, dry wood, nonconductive plastics, most textiles, are substantially none absorbing and have modest refractive indices (ε_R 2–4) for 900-MHz radio waves (DOBKIN, 2013).

Metals reflect essentially all the radiation that falls upon them. Water, with a dielectric constant of around 80, also reflects almost all of an incident wave and absorbs most of the rest (AHSON, 2008).

The dielectric plays especially in the UHF RFID frequency range an important role, as the information transmission mainly takes place over the far field, where the electrical component (opposed to the magnetic component) is predominating.

The electrical flux density D is depending on the electric field E and the permittivity of the media ε. The permittivity can be considered as a scalar or a tensor, the D and the E field are parallel, see equation 4.

$$D = \varepsilon \mathrm{E} = \varepsilon_0 \varepsilon_R \mathrm{E} \tag{4}$$

ε_0 denotes the vacuum permittivity and ε_R the dielectric constant of the transmission media.

According (DOBKIN, 2013), a label antenna applied on a carrier material of a high dielectric constant, has to be able to handle two effects, in order to keep a good performance:

- Detuning of the label resonance frequency will lead to mismatch and to performance loss. It needs a dedicated antenna design for high dielectric carriers.
- Depending on the imaginary part of the dielectric constant of the media (carrier material), a certain amount of UHF waved will be absorbed and reduce as well the read range (attenuation).

C. Reflection

As described by (BALANIS, 2005), a pure reflection of the traveling wave will conserve energy of the field. Wave-guides are an example of devices that uses these pure reflections for transmission. Multipath wave propagation leads to constructive or destructive interferences – one of the unwanted phenomenon is in the UHF area. There are two different kinds of reflection. The directional reflection occurs on plain surfaces and the diffuse reflection occurs on rough surfaces Figure 7.

Figure 7 - Constructive and destructive interferences
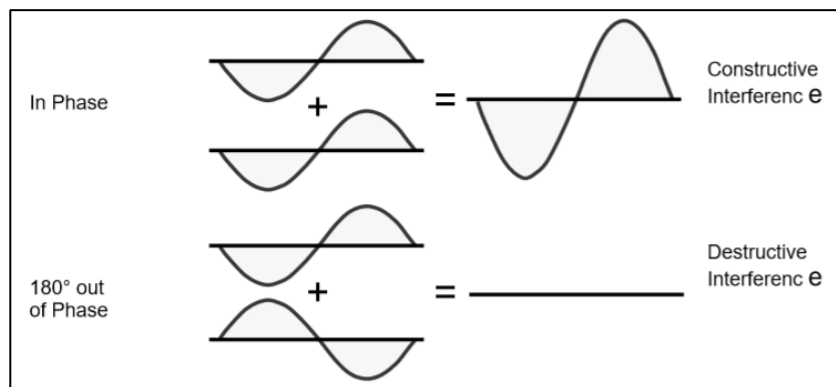
Source: BALANIS, 2005.

D. Diffraction and Refraction

When a wave passes from one medium into another medium that has a different velocity of propagation, a change in the direction of the wave will occur. This changing of direction as the wave enters the second medium is called refraction (BALANIS, 2005).

Diffraction is the bending of a wave around objects or the spreading after passing through a gap, Figure 8. It is due to any wave's ability to spread in circles or spheres in 2D or 3D space. Huygens' Principle is based on this process. In 1678, the great Dutch physicist Christian Huygens (1629-1695) wrote a treatise called 'Traite de la Lumiere' on the wave theory of light, and in this work he stated that the wave front of a propagating wave of light at any instant conforms to the envelope of spherical wavelets emanating from every point on the

wave front at the prior instant (with the understanding that the wavelets have the same speed as the overall wave).

Figure 8 - Diffraction
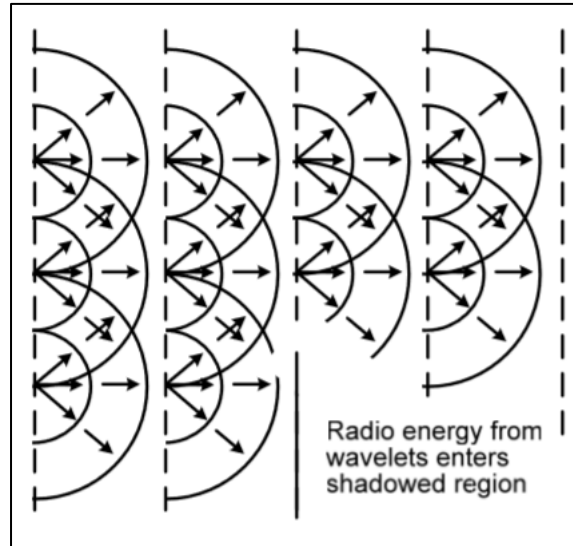
Source: BALANIS, 2005.

E. Polarization

According (BALANIS, 2005), the orientation of the electrical field component of an electromagnetic wave determines its polarization. There are three different polarizations possible, Figure 9. An elliptical polarization has an elliptical electrical field vector in the plane perpendicular to the propagation direction. Additionally, there are the special forms of circular- and linear polarization.

Figure 9 - Linear, circular and elliptical polarization
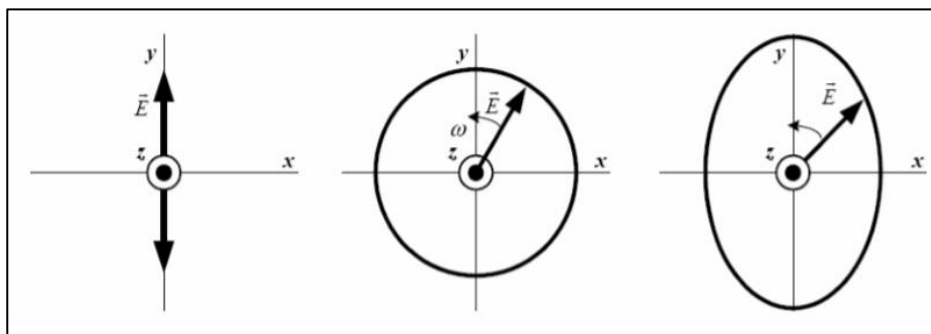
Source: BALANIS, 2005.

Depending on the rotation direction of the circular polarization it is called left or right circular polarized, where right means clockwise. In linear polarization, the electrical field vector has a relation to the earth's surface. Depending on this orientation one can differ between two forms of linear polarization. The horizontal polarization, where the electrical field vector is aligned parallel to the earth's surface, and the vertical polarization, where the electrical field vector is perpendicular to the earth's surface. In circular polarization, the wave front appears to rotate every 90 degrees between vertical and horizontal, making a complete 360-degree rotation once every period, Figure 10.

Figure 10 - E-field vector projection of a circular polarization
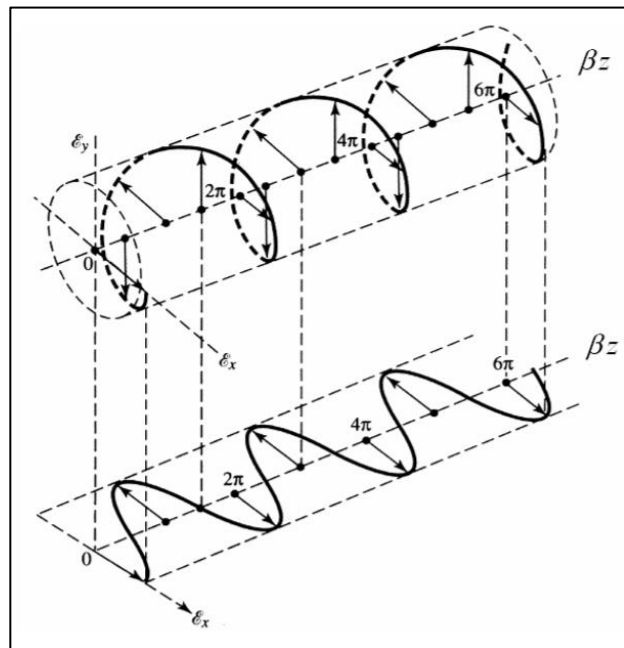
Source: BALANIS, 2005.

The power transfer depends on the orientation of the receiving and transmitting antenna, Figure 11. Linear polarized antennas (horizontal or vertical) have 0dB loss if they are oriented in the same plane. If one antenna is linear and the other circular polarized the loss is always 3dB. However if a linear polarized label antenna (dipole) points direct longitudinal towards a reader antenna no power is transferred and the loss is infinite.

Figure 11 - Polarization mismatch

Source: BALANIS, 2005.

If the orientation of the two polarizations (label and reader) is considered in the vector plane, the efficiency of the power transfer (tag → reader / reader → tag) depends on how much the vector directions overlap. The non – overlapping components will result into losses (BALANIS, 2005).

2.2.2 Fundamental Antenna Parameters

In this section the key characteristics of an antenna are described and also the equivalent circuits of the system tag antenna.

A. Radiation Pattern

An antenna radiation pattern or antenna pattern is defined as a mathematical function or a graphical representation of the radiation properties of the antenna as a function of space coordinates (BALANIS, 2005).

The output characteristic of an antenna is described by the radiation pattern, which is the relative distribution of the radiated power as a function of the direction in space. Even if the radiation pattern is 3 dimensional very often only planar sections (cuts) are presented, Figure

12. The two most important views are those of the principal E-plane and H-plane patterns. The first one is a view of the radiation pattern obtained from a section containing the maximum value of the radiated field and in which the electrical field lays in the plane of the chosen sectional view. The later plane pattern is a sectional view in which the H field lies in the plane of the section, and this section is chosen to contain the maximum direction of radiation.

Figure 12 - Radiation pattern
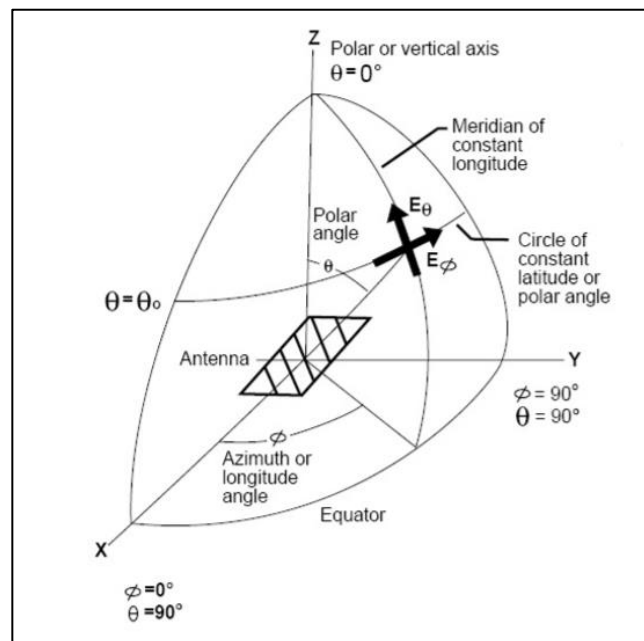
Source: BALANIS, 2005.

B. Field Regions

At high frequency measurements in the UHF region (and beyond) parasitic effects do play an increasing important role. In particular for radiating structures as e.g. antennas it is getting more difficult since every conducting- or non-conducting material (with a dielectric constant and/or a permeability constant greater than 1) located in the reactive near-field region causes changes of the boundary condition of the antenna (modifying the coupling between the antenna elements) and therefore changes its characteristic (DOBKIN, 2013).

According (BALANIS, 2005), in general the space around a radiating element (e.g. an antenna) is divided into three different regions, Figure 13: The reactive near field region, the radiating near field (Fresnel) region, and the far field (Fraunhofer) region.

Figure 13 - Field regions around an antenna
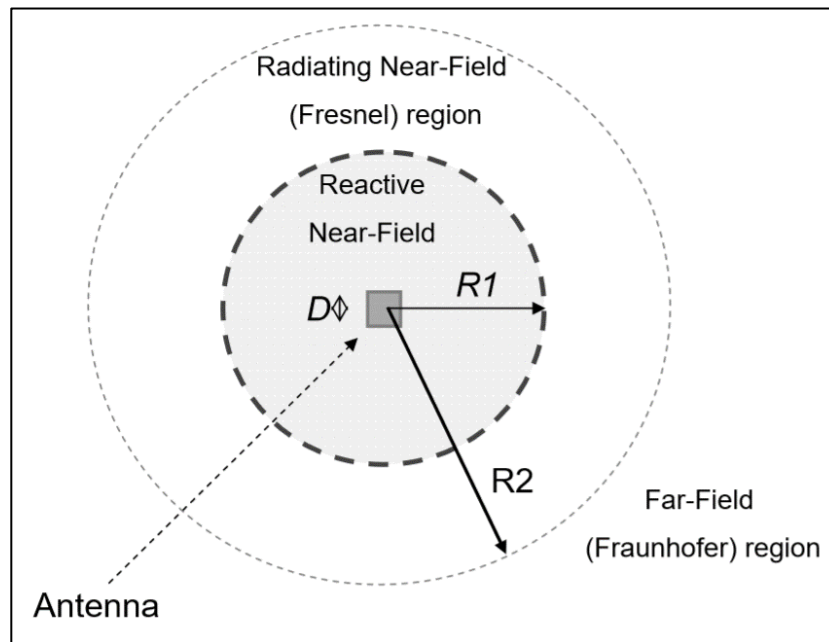
Source: BALANIS, 2005.

Whereas D is the largest dimension of the antenna, and R denotes the distance.

- **Reactive Near Field Region**

Reactive near field region is defined as that part of the near field region immediately surrounding the antenna wherein the reactive field predominates (BALANIS, 2005).

A commonly used formula for the boundaries of the reactive near field region is:

$$R_1 \leq 0.62\sqrt{\frac{D^3}{\lambda}}$$

The field decays rapidly in the order of $1/R^4$.

Radiating Near Field Region

The radiating near field region, also known as Fresnel region, is located between the reactive near field region and the far field region (BALANIS, 2005).

The boundaries are defined as follows:

$$0.62\sqrt{\frac{D^3}{\lambda}} \leq R_2 \leq \frac{2D^2}{\lambda}$$

If an antenna has a maximum dimension that is not large compared to the wavelength, this region may not exist.

Far Field Region

According (BALANIS, 2005), the relative angular distribution does not vary with distance in the far field region. The radiated power from an antenna decays in the far field region according to the inverse square law $(1/R^2)$ as a function of the distance. The far field region, also known as Fraunhofer region, is defined for distance:

$$R \geq \frac{2D^2}{\lambda}$$

C. Input Impedance

The input impedance is the parameter, which describes the antenna input behavior as a circuit element. As usual in electronic circuit design it is important to match this input impedance ($\underline{Z}_{antenna}$) to a given source impedance, which is in case of RFID applications usually the chip impedance of the transponder IC ($\underline{Z}_{Chip}$). The maximum power delivered from the source to the antenna is given if the antenna input impedance is complex conjugate to the chip impedance (DOBKIN, 2013).

In practical, the better the matching, the less power is reflected on the connection between IC bumps and label antenna pads. This will result in a maximum power transfer to the integrated circuit (IC). An UHF RFID IC is an ultra-low power design, therefore matching is essential in order to make the good sensitivity of the IC result in excellent read ranges in an end application (DOBKIN, 2013).

D. Radiation Resistance

The radiation resistance of an antenna is equivalent to a resistance that would dissipate the same amount of power as the antenna radiates, when the current in this resistance is equal to the current at the antenna input terminals (BALANIS, 2005).

The total resistance of an antenna ($R_{antenna}$) can be separated into a series circuit of two different resistors, equation 5.

$$R_{antenna} = R_{rad} + R_{loss} \tag{5}$$

Where R_{rad} is the radiation resistance and R_{loss} is the loss resistance representing the unwanted losses caused by the non-perfect conductors and (substrate) materials.

Accordingly, one can further separate this loss resistance into those two contributions, equation 6.

$$R_{loss} = R_{loss,con} + R_{loss,sub} \tag{6}$$

E. Gain and Directivity

The ratio of the radiation intensity in any direction d to the intensity averaged over all directions is the directive gain of the antenna in that direction. The directive gain along the direction in which that quantity is maximized is known as the directivity of the antenna. The directivity of the antenna multiplied by the radiation efficiency is the gain of the antenna (BALANIS, 2005).

In the direction of maximum radiated power density, we get G times more power that we would have obtained from an isotropic antenna.

The gain of an antenna gives its ability to focus the radiated power in a particular direction relative to an isotropic point source and is given by:

$$Gain = 4\pi r^2 \left(\frac{S}{P_{in}}\right) \tag{7}$$

The far field power density S (equation 8) can be calculated using the equation 7:

$$S = \frac{Pin.Gain}{4\pi d^2} \left[\frac{W}{m^2}\right] \tag{8}$$

Pin: Average power at antenna [W];

Gain: Numerical gain;

d: Distance from antenna [m].

More generally the gain is related to the directivity of the antenna by the efficiency of the antenna e

$$G(\theta, \phi) = eD(\theta, \phi) \tag{9}$$

Where D is given by

$$D(\theta, \phi) = \frac{power\ radiated\ in\ a\ fixed\ direction(\theta, \phi)}{total\ power\ radiated\ by\ the\ antenna} \tag{10}$$

In national UHF frequency regulations, radiated power is defined with different terms in the different countries.

F. Efficiency

The efficiency of an antenna takes into account the influence of additional losses, which may occur at the input terminals or within the structure of the antenna (BALANIS, 2005).

It is the percentage of the power delivered to the antenna that actually gets radiated as opposed to being absorbed or reflected.

For an ideal, lossless antenna, the gain equals the directivity, equation 9.

Practically, these can be losses due to reflection (mismatching between the IC and the antenna), or conduction and/or dielectric losses (DOBKIN, 2013).

G. Bandwidth and Q

The bandwidth can be considered to be the range of frequencies, on either side of a center frequency (for example the resonance frequency of a dipole), where the antenna characteristics (such as input impedance, pattern, beam width, polarization, side lobe level,

gain, beam direction, radiation efficiency) are within an acceptable value of those at the center frequency (BALANIS, 2005).

According (BALANIS, 2005), an antenna simultaneously stores charge (capacitance), opposes changes in current (inductance), and radiates power into the wide world (resistance). From the electrical point of view, an antenna looks like an R-L-C circuit. The configuration of the circuit depends on the antenna type. A dipole that is short compared to the wavelength looks like a series combination of an inductor and capacitor with some resistance, Figure 14. The inductance and capacitance are both roughly proportional to the length of the dipole.

In general, the bandwidth is inversely proportional to the Q factor, which is the ratio of the total reactance to the resistance ($BW \sim 1/Q$). For a simple series resonant circuit, Q is about twice the voltage amplification factor. Thus, voltage amplification must be traded against bandwidth. Antennas with large reactance (that is, large values of inductance and small values of capacitance) and small values of resistance may be adjusted to be matched to the tag at one frequency, with good power transfer and voltage multiplication, but performance will degrade at other frequencies. Antennas with small reactance will provide better performance over frequency.

H. Electrical equivalent circuits

For UHF antenna design, it is necessary to investigate the impedances of the system components, meaning, IC, assembly, and tag antenna (DOBKIN, 2013).

• Equivalent circuit of the IC

Electrically, a passive UHF RFID IC can be depicted as a complex, capacitive impedance (DOBKIN, 2013). Figure 14 shows the equivalent circuit of the input impedance. The impedance value of a UCODE IC is given in the datasheet (NXP, 2017) and also corresponds to the shown serial equivalent circuit.

Figure 14 - Equivalent circuit of IC input impedance
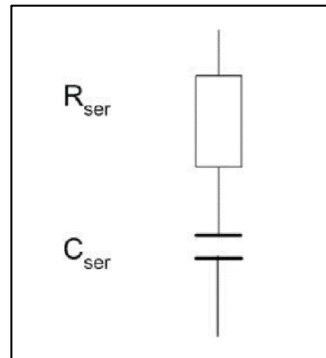
Source: DOBKIN, 2013.

For the parallel circuit, the values of the real and imaginary part would change (DOBKIN, 2013).

- **Equivalent circuit of the assembled IC**

At each assembly process, parasitic capacitances and resistors are inherited, which result in an additional parallel impedance, Figure 15 (DOBKIN, 2013). The value depends on assembly process and parameters.

Figure 15 - Serial equivalent circuit of assembled IC
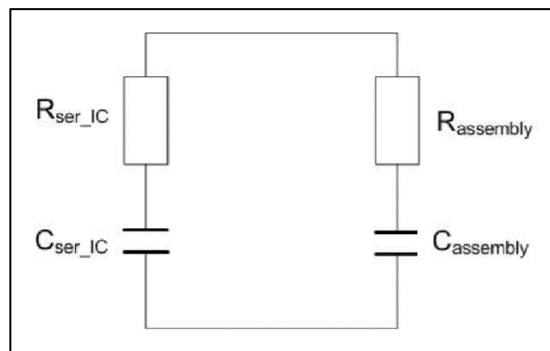
Source: DOBKIN, 2013.

- **Equivalent circuit of a loop antenna**

According (DOBKIN, 2013), since the magnetic loop is quite small compared to the wavelength, its near-field components are mainly magnetically. Due to that fact, its reactance is quite insensitive to materials with different electrical permittivity in its close proximity.

The reactance of the magnetic loop can be simply modeled by an inductor. Together with the input capacitance of the IC, an LC-resonating circuit is formed as shown in Figure 16.

The real part of the impedance of the magnetic loop consists of its radiation resistance and an additional resistance representing the losses of the loop antenna. The radiation of a loop-antenna depends on its area relative to the wavelength at the operating frequency.

Figure 16 - Equivalent circuit magnetic loop
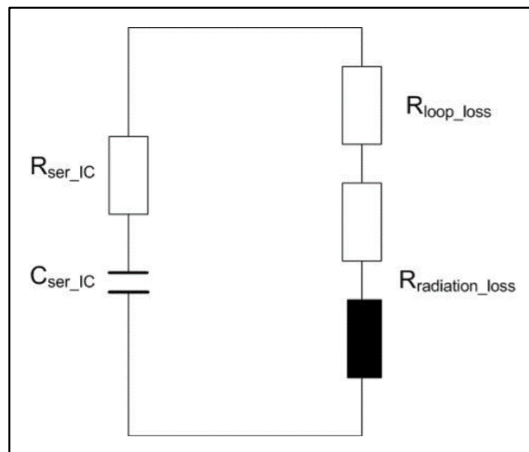
Source: DOBKIN, 2013.

- **Equivalent circuit of a broadband dipole**

A conductor always has a capacitance and an inductance. Hence a dipole in a homogenous electromagnetic field can be represented by a series-L-C resonant circuit, Figure 17 (DOBKIN, 2013).

Figure 17 - Equivalent circuit of a dipole
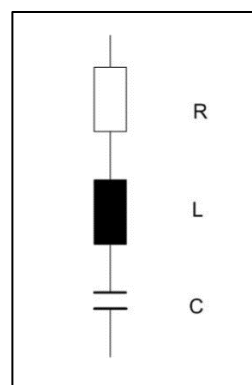
Source: DOBKIN, 2013.

The resonance frequency of such a circuit is determined by:

$$\omega_{res} = \frac{1}{\sqrt{LC}} \tag{11}$$

At a given resonance frequency, the product of L and C will result in a certain fixed value. Although the product is fixed the relation of L/C can be chosen arbitrarily. As an example, doubling C and halving L will result in the same resonance frequency. This gives some freedom in the design of the dipole, which means that it is possible to design various kinds of dipoles with different shapes, which all have the same resonance frequency (DOBKIN, 2013).

The difference between 2 dipoles with the same resonance frequency but a different L/C-ratio is the quality and hence the bandwidth, since

$$Q \sim \sqrt{\frac{L}{C}} \tag{12}$$

And

$$BW \sim \frac{1}{Q} \tag{13}$$

Therefore the L/C-ratio has to be minimized in order to obtain a high bandwidth of the dipole. As an example, increasing the thickness of a dipole can achieve this. The increased thickness reduces the self-inductance and the increased surface of the dipole results in an increased capacitance of the dipole (DOBKIN, 2013).

I. Matching

The input impedance is the parameter, describing the antenna input behavior as a circuit element. As usual in electronic circuit design it is important to match this input impedance ($\underline{Z}_{antenna}$) to a given source impedance, which is in case of RFID applications the chip impedance of the transponder IC ($\underline{Z}_{chip}$). The maximum power delivered from the source to the antenna is given if the antenna input impedance is complex conjugate to the chip impedance:

$$\underline{Z}_{antenna} = \underline{Z}_{chip}^{*} \tag{14}$$

Separated into real and imaginary parts we get the following conditions:

$$R_{antenna} = R_{chip} \tag{15}$$

$$X_{antenna} = -X_{chip} \tag{16}$$

According (DOBKIN, 2013), for designing an efficient antenna it is necessary to match the real part and the conjugate imaginary part of the source impedance (practically this takes into account the IC impedance and the parasitic assembly impedance). Assuming complex conjugate impedance matching between antenna and chip (assembled) and further assuming the case of a receiving antenna the maximum power delivered from the antenna ($P_{antenna,max}$) is:

$$P_{antenna,max} = \frac{|V_{antenna}|^{2}}{4R_{antenna}} \tag{17}$$

Where $V_{antenna}$ is the voltage generated by the label antenna due to receiving an electromagnetic wave and $R_{antenna}$ is the resistance of the label antenna.

In order to estimate the variation of the read range of a given transponder if the loss impedance is being modified (caused by modifications of the flip chip mounting parameters) the following approach can be followed:

The received (tag) power at an arbitrary point is:

$$P_{Tag} = A_{Tag}.S \tag{18}$$

with:

A_{Tag} = Effective Area of the (tag) antenna (derived from radar technique)

S = Power density.

Further it is:

$$A_{Tag} = \frac{\lambda_0^2}{4\pi}.G_{Tag} \tag{19}$$

with:

λ_0 = wave length ($\lambda_0 = c/f_0$)

G_{Tag} = gain of tag antenna

And

$$S = \frac{P_{Reader} \cdot G_{Reader}}{4\pi D^2} \tag{20}$$

with:

P_{Reader} = reader/scanner power,

G_{Reader} = gain of reader antenna and

D = maximum distance between tag and reader.

Using Equation 18 and Equation 19 in Equation 20 and solving for the distance D yields:

$$D = \frac{\lambda_0}{4\pi} \sqrt{\frac{P_{Reader}}{P_{Tag}} \cdot G_{Reader} G_{Tag}} \tag{21}$$

It can't calculate the new distance (which is reduced since energy is short circuited by the loss impedance parallel to the chip) in relation to the maximum theoretical distance. Defining the relative change of the distance yields:

$$\Delta D = \frac{D - D_0}{D_0} \tag{22}$$

Using Equation 21 with $P_{Reader} = P_0$ and $P_{Tag} = P$ respectively yields:

$$\Delta D = \sqrt{\frac{P_0}{P}} - 1 \tag{23}$$

Further the total power received by the tag consists of three terms:

$$P_{Tot} = P_{Chip} + P_{loss} + P_{antenna} \tag{24}$$

The related efficiency for the IC will result in:

$$\eta_{Chip} = \frac{P_{Chip}}{P_{Tot}} = \frac{P_{Chip}}{P_{Chip} + P_{loss} + P_{antenna}} \tag{25}$$

Regarding the total received tag power (P_{Tot}) it is necessary to differ two cases:

a) Ideal case

Theoretical maximum distance with no losses and optimum impedance matching between antenna and chip, which yields:

$$P_0 = P_{Tot} = P_{Chip} + P_{loss} + P_{antenna} \qquad (26)$$

With $P_{loss} = 0$ (no losses) and $P_{Chip} = P_{antenna}$ (power matching) it gets:

$$P_0 = 2 . P_{Chip} \qquad (27)$$

b) Real case

Taking into consideration the parallel loss impedance, which yields:

$$P = P_{Tot} = \frac{P_{Chip}}{\eta_{Chip}} \qquad (28)$$

Using equation 25 and equation 26 in equation 22 yields the change in the distance between label and reader in relation to the theoretical maximum range:

$$\Delta D = \sqrt{2 . \eta_{Chip}} - 1 \qquad (29)$$

The matching system is shown by a simplified equivalent network consisting of the chip, the loss impedance, and the antenna (including an ideal voltage source). Figure 18 shows the related network. The elements of the transponder are substituted by series circuits of resistors and capacitors (chip and loss impedance) and a resistor and an inductance (antenna). All elements are parallel connected. The voltage source V_Antenna represents the voltage of the antenna generated by the received electromagnetic wave.

Figure 18 - Equivalent electrical circuit of a transponder
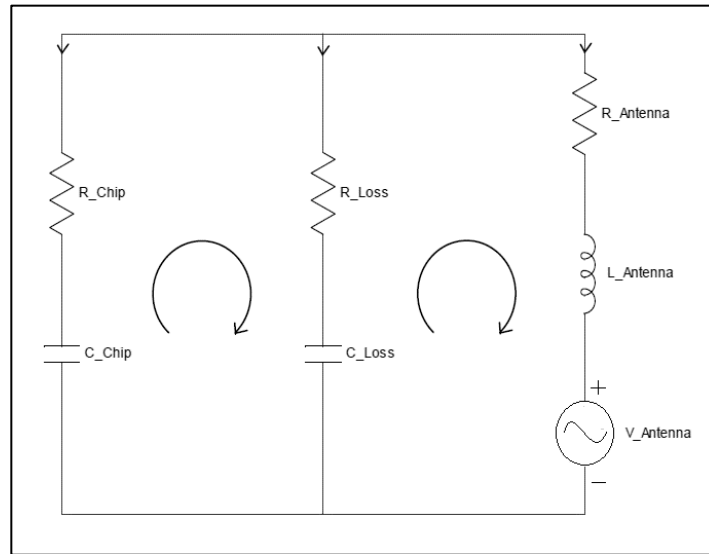
Source: Prepared by the author, 2019.

J. Reflection coefficient

According (BALANIS, 2005), especially at high frequencies such as e.g. UHF the mismatch between a source and a load (or in general between to elements) is represented by the reflection coefficient $\underline{\Gamma}$.

Based on transmission line theory this reflection coefficient is defined by the ratio of the reflected wave to an incident wave. Hence the reflection coefficient is simply a measure of the quality of the match between the source- and the load impedance. Therefore, the dimension less complex reflection coefficient is defined by:

$$\underline{\Gamma} = \frac{\underline{Z} - \underline{Z}_0^*}{\underline{Z} + \underline{Z}_0} \tag{30}$$

Where $\underline{Z}$ is the measured impedance and $\underline{Z}_0$ is the normalizing impedance.

Very often the imaginary part of $\underline{Z}_0$ is zero (or can be neglected) and the real part is fixed to $R_0 = 50\Omega$, which results in a reflection coefficient of:

$$\underline{\Gamma} = \frac{\underline{Z} - R_0}{\underline{Z} + R_0} \tag{31}$$

Furthermore, the reflection coefficient is usually given as a logarithmic data (in dB):

$$\Gamma_{dB} = 20 \log(|\underline{\Gamma}|) \tag{32}$$

The above equation has to be used for amplitudes like e.g. voltages. Whereas the factor 20 has to be replaced by the factor 10 if powers i.e. square of amplitudes are considered.

Another derivation of the reflection at a port of a device is based on the network analysis theory of a two-port device (or network) and its related scattering parameters.

Two-port s-parameters are defined by considering a set of voltage waves. Those voltage waves are being divided by the square root of reference impedance. If further the square of the magnitude of these new variables is being considered one gets traveling power waves:

$|\underline{a_1}|^2$ = incident power wave at the network input

$|\underline{b_1}|^2$ = reflected power wave at the network input

$|\underline{a_2}|^2$ = incident power wave at the network output

$|\underline{b_2}|^2$ = reflected power wave at the network output

These variables are related in the following equation system:

$$b_1 = a_1 . s_{11} + a_2 . s_{12} \tag{33}$$

$$b_2 = a_1 . s_{21} + a_2 . s_{22}$$

A two-port network with its related power waves is presented in Figure 19.

Figure 19 - Two-port network with wave-parameter
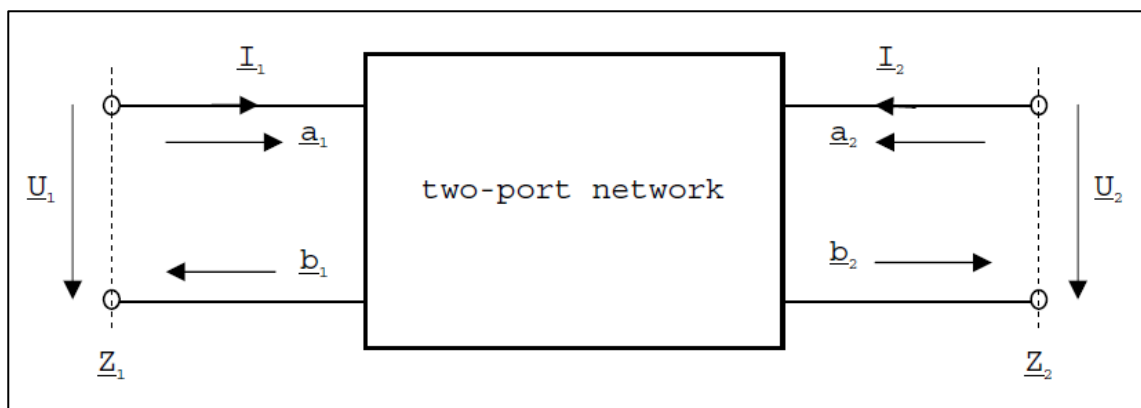
Source: BALANIS, 2005.

Terminating the output of a two-port device with the reference impedance causes no reflection at the output and hence $\underline{a}_2$ is zero, then we get:

$$\underline{s}_{11} = \left.\frac{b_1}{\underline{a}_1}\right|_{a_2=0} \equiv input \ refletion \ coefficient \tag{34}$$

$$\underline{s}_{21} = \left.\frac{b_2}{\underline{a}_1}\right|_{a_2=0} \equiv forward \ transmission \ coefficient$$

Driving the two-port device (or network) from the output terminal and terminating the input port with the reference impedance causes no reflection at the input and hence $\underline{a}_1$ is zero, then we get:

$$\underline{s}_{22} = \left.\frac{b_2}{\underline{a}_2}\right|_{a_1=0} \equiv output \ refletion \ coefficient \tag{35}$$

$$\underline{s}_{12} = \left.\frac{b_1}{\underline{a}_2}\right|_{a_1=0} \equiv reverse \ transmission \ coefficient$$

Per definition the scattering parameter $\underline{s}_{11}$ is equal to the reflection coefficient $\underline{\Gamma}$ as described above. Usually the scattering parameters are also given in decibel (dB).

The traditional way to determine the reflection coefficient ρ is to measure the standing wave caused by the superposition of the incident wave and the reflected wave. The ratio of the maximum divided by the minimum is the Voltage Standing Wave Ratio (VSWR). The VSWR is infinite for total reflections because the minimum voltage is zero.

If no reflection occurs the VSWR is 1.0. VSWR and reflection coefficient are related as follows:

$$VSWR = \frac{(1+|\rho|)}{(1-|\rho|)} \tag{36}$$

Most present instrumentation measures the reflection coefficient and calculates the VSWR.

K. Tuning of an Antenna

Taking into account the described matching technique and the impact of each part on the matching between antenna and IC, following parameters can be used to tune the antenna:

- Loop size

- Dipole length

- Bandwidth

The parametric read range of the tag is defined in function of the loop dimension; the length of the dipole; and the distance D, Figure 20.

Figure 20 - Prototype antenna tuning
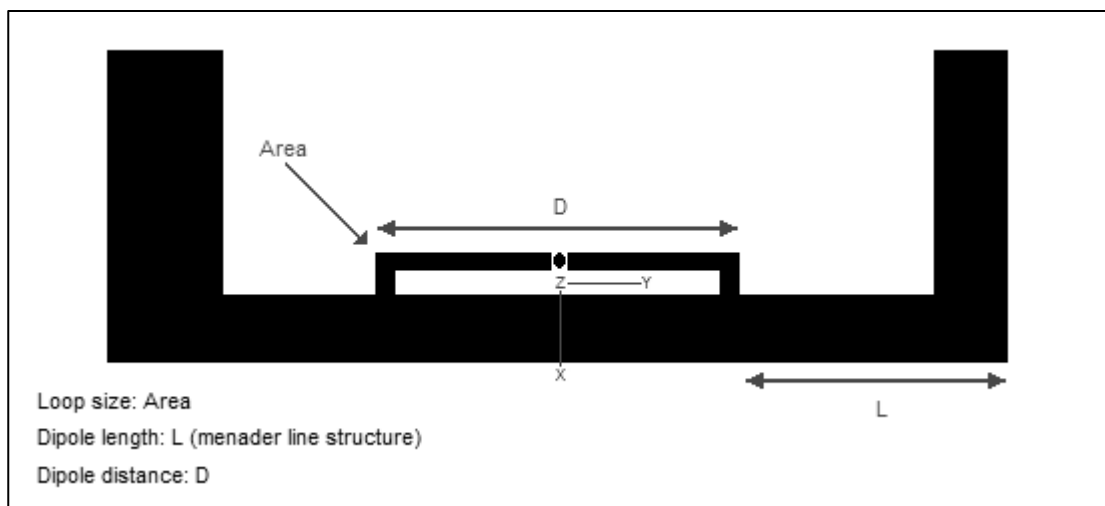
Source: Prepared by the author, 2019.

According (DOBKIN, 2013), the tuning of the antenna will change by increasing the loop dimension or reducing the total length of the dipole (obtained by modifying the line). An increasing of the loop dimension will decrease the lower resonance frequency (loop resonance) of the tag antenna. A reduction of the total length L of the dipole will increase the upper resonance frequency (dipole resonance) of the tag antenna.

Variation on the distance D between the connection points of the two half dipoles to the loop will allow to vary the in frequency the two main resonances of the tag antenna (loop and

dipole, by increasing or reducing the antenna bandwidth). A small distance between the dipole arms implies close resonance frequencies and small bandwidth. High separation distances imply higher separation in frequency between the two resonances and higher bandwidths. A high distance can create a low performing frequency region between the two resonance frequencies.

3 PROBLEM STATEMENT

Several technologies have already been implemented in the search for the best way to record the number of passengers transported. At the beginning it was the driver himself who registered the presence of a new passenger, but with the increase of population and consequently increase of passengers, this management was unsustainable and the need to apply engineering to solve the problem.

3.1 IMPLEMENTED TECHNOLOGIES CURRENTLY IN USE

The following are the main forms of passenger registration used in public transport vehicles.

3.1.1 Turnstile

The turnstile, also known as baffle gate, is a device for recording the flow of people. In public transport the turnstile is used to account for passengers who have been in the vehicle during a journey. Its constructive form allows the passage of only one person being counted through the rotating movement of the device, Figure 21. It is considered one of the first engineering devices used in public transport vehicles focused on passenger counting (MONTHLY, 1923).

Figure 21 - Turnstile

Source: UPSECURE website[1].

Despite being a reliable device in passenger counting, its geometry, besides reducing the internal space of the vehicle, makes it impossible to install near the boarding door.

3.1.2 Infrared Barrier

Another technology used to account for passenger flow is the infrared barrier. Consisting of a transmitter and a receiver it create a punctual ray and operate as on/off detection. According (PINNA, 2010), the infra-red emitters are generally set parallel to one another so that the Light Emitting Diode (LED) interruption occurs in the direction of crossing and the entry direction can thus be discriminated from the exit one: because of their bar configuration, this type of infra-red sensor is also defined as barrier sensors, Figure 22.

Figure 22 - Infrared barrier

Source: Intelligent Transport website[1].

The barrier sensors, unlike the turnstiles, can be installed at the boarding and disembarking door, but their passenger counts are less effective. Because they are on / off sensors, they allow passengers to pass in parallel or even queued without be counted. For this, it is enough that the light beam continues being obstructed.

---

[1] Available at: <https://www.intelligenttransport.com/transport-articles/3116/automatic-passenger-counting-systems-for-public-transport/>. Access in: 17 Feb. 2018.

3.1.3 Vision Solutions

Visual solutions are based on optical technologies, i.e. they manage to detect the shapes of the passengers and distinguish them from other ones; they also detect their moving direction and subsequently identify either the entry or the exit movements (PINNA, 2010), Figure 23.

As regards, the vision systems, on the market there are different solutions, but almost all are based with two stereoscopic cameras able to capture images in the area below the devices. These systems, mounted above the doors, are able to count passengers entering or leaving buses, trams or trains with a high accuracy. Those systems generally have integrated LEDs, which enable the system to operate in almost any kind of lighting condition. An adjustable counting threshold allows through measurement of passenger heights the distinction to be made between children and adults.

Figure 23 - Vision solution

Source: Youtube page[1].

According to (CHEN, 2012), with the improvement of the algorithms used in image processing it is possible that in a short time we will have market solutions with effective passenger accounting. Because it is a cost-effective solution, its use is still restricted.

---

[1] Available at: <https://www.youtube.com/watch?v=s6sEhpEmLQU>. Access in: 17 Feb. 2018.

3.2 ADVANTAGES AND DISADVANTAGES OF THE IMPLEMENTED TECHNOLOGIES CURRENTLY IN USE

The mentioned technologies have advantages and disadvantages, and are not unanimous in the market, so there is a gap for the emergence of new ideas that can reach a greater number of adepts.

In an interview given by Mr. Nilo Borges, Director of Acquisition and Logistics at Marcopolo, a Brazilian company that is leader in the bus market, during a lunch meeting at CIC in Caxias do Sul / RS, the most relevant aspects to the market are: quality, performance, availability and cost effectiveness.

Quality and availability are characteristics that can be achieved by any technology, so it is important that the company that manufactures the product meets the demands of the market. Already performance and cost are very points related to technology, concludes the Director.

Based on the passenger count, turnstile is the technology with the most effectiveness of the three presented, but to guarantee this performance it is necessary a physical structure that obliges the passenger to pass through it, reducing the space of the internal vehicle. Due to its physical structure, the installation is restricted to the central region of the vehicle, thus allowing the passenger to travel before passing through it, that is, without actually being counted. This model of passenger management is not seen by the Automatic Fare Collection (AFC) as an acceptable alternative in the context of smart cities.

Another technology that has also lost strength is infrared barriers. Despite being accepted as one of the technologies adopted by the AFC, the technology has already proved problematic in populous cities. As already mentioned, passengers embarking or disembarking in parallel or in a row, but without a distance that allows the beams of lights to pass from one

tower to another, makes the count is incorrect. The positive factor of this technology is to be the lowest cost effective in the market.

The third technology mentioned in this work are image processing techniques. It is the technology pointed out by the AFC as the great bet for the accounting of passengers by allowing not only the counting but also the possible recognition of the passenger, but still presents high costs that make it little present in the present day, so the market is still open to new technologies.

3.3 FACTORS THAT HINDER THE PASSENGER COUNT

The correct count of the passenger's number is theoretically simple to perform, but in practice there are a number of factors that end up limiting the effectiveness of the solutions presented in the market. The following are some of the most significant factors that are considered obstacles in this scenario.

- In order to facilitate the flow of passengers, the areas for installation of reading equipment are restricted;

- The variability of passengers is large, so several characteristics are random such as height, width, physiognomy, type of clothes and etc.;

- Controlling the crossover velocity of the passenger by a reader element can lead to a decrease in transport productivity, so it is a factor that should also be considered random;

- Because it is a vehicle with a high flow of passengers, it is not advisable to limit the number of individuals that will pass through the reader at the same time.

3.4 THE PROPOSAL

The radio frequency identification is not a new technology, but has evolved much in recent years, and today it is present in a number of market applications (MALISON, 2008).

Basically, it is used in two difference frequency bands: 860-915 MHz to UHF and 13.56 MHz to HF. The HF models are applied where the exchange of information needs to be done with security or when there is greater data storage. The UHF models are present in applications where it is necessary to make the communication to distances over 10 cm. The use of this technology is so large and varied that the control and management of the communication process between transceiver and transponder is performed by standard protocols such as ISO 15693 and ISO 1800-3 to HF or ISO 18000-6 and EPC to UHF.

One of the possible applications of RFID is the identification and tracking of public transport users (SENNOU, 2013). With this identification and tracking application it is also possible to analyze the trajectory or origin and destination of passengers, creating an intelligent transport system (GHASEMZADEH, 2014). In order to preserve user privacy issues, data analysis takes place in the general context of the use of public transport and not the trajectory of each passenger. This type of intelligent transport system is called Automated Fare Collection and is being widely used in public transport in many parts of the world (NUNES, 2016). As (ZÖSCHER, 2015) states, the AFC system has been a crucial element for the growth of the effectiveness of public transport networks. AFC system can generate an integrated ticketing system in the different modes of public transport (NUNES, 2016). Another advantage of this system is the type of user ID, how old he/she is, if the person is a student or an ordinary user, and like this it can generate the discounts required for each type of user (GHASEMZADEH, 2014). In (CHENG, 2016), a study about the usage of smart cards in transit systems is presented, particularly focusing in multipurpose cards, highlighting the importance of this topic for intelligent transport systems.

The work (MALISON, 2008) is focused in these aspects of new applications for RFID. He has characterized the implementation of RFID system for detecting people because the rapid growth of the population is demanding the development of identification and location

techniques of individuals. The work presented in (MALISON, 2008) provides the basis for the proposal of this current paper. Malison discusses the use of two directional antennas pointed towards the target producing a full scan and allowing tag detection in different parts of the human body. The Malison's experimental results contribute to understand the related reading loss and the power required for effective recognition of the tags, although it is based on the use of frequencies above 2 GHz.

Another relevant research in the area that also contributed to this current study is presented in (OBERLI, 2010). This work shows the implementation of a personal recognition system in the form of a portal that detects UHF RFID tags inserted in passenger charging cards. The use of volunteers, carrying cards in different parts of the body (Handheld, Wallet-Backpack, Wallet-Pocket, Loose-Pocket), allowed the researchers to conclude that cards with two tags of different RFID frequencies lead to a loss of 18% in recognition. On the other hand, cards with only the UHF RFID tags have a recognition rate of 91%. They also found that the use of two reader antennas increases in 10% the recognition of the tag, while three or four antennas represented an additional increase of maximum 2%. The authors state that the line of sight and the pattern of the antenna radiation are aspects of great importance to the recognition system performance, and may not be neglected.

The studies (MALISON, 2008; OBERLI, 2010; TSAI, 2012) presented results that contributed to the scientific community, but left large gaps to be worked, especially in the pursuit of better performance regarding the relationship between tags and readers' antennas.

Looking for a better performance, this thesis is focusing on two specific aspects: the elaboration of a tag of better performance and the redefinition of positioning of the reader antennas. This work evaluates the performance of the suggested tag in front of three commercial RFID UHF tag models, always considering the additional use of an HF payment RFID tag coupled to the card. People of different physical biotypes carry RFID cards randomly

distributed in different places, such as in the front or back pocket, handheld, in the wallet, etc. The possible variations in the way people carry these tags will be further defined. Systems with up to four directional antennas are assembled in order to find the best transit area of the scan configuration. These tests provide a basis for decision about the type of tag, as well as the best positions for the readers' antennas.

This proposal aims to reach a level of passenger recognition of more than 80%, an index considered acceptable by the AFC for passenger traffic management.

4   STUDY METHODOLOGY

The solution proposed in this thesis focusing on the AFC is to use RFID cards to detect users and charging. The question is that the human body is primarily composed of water which directly affects the reading of RFID tags, as highlighted by (MALISON, 2008). (MALISON, 2008; TSAI, 2012) evaluated in different contexts the human body influence in reading the tags and proposed different ways to minimize the detected problems. In the same period (OBERLI; 2010) conducted tests idealizing the detection of users by passing through a portal reader.

Following the previous works, this thesis presents the proposal of a new tag to be applied to the validation card of the passenger and a similar concept of (OBERLI, 2010) portal, but with a different carrying scenarios and situations.

Based on an informal survey of 120 public transport users in Porto Alegre / RS, a scenario of tag carrying positions is generated to evaluate the performance of the proposed tag and the concept of distribution of reader antennas in a real context of use in Brazilian public transport.

In the first considered scenario, two volunteers from different biotypes pass through the portal with four reading antennas positioned at 0° (Figure 25a) and carrying the UHF tags in different positions, according the details shown in the survey. With the portal configured as indicated by (OBERLI, 2010) and illustrated in Figure 24, the volunteers take the first tag template and pass by the portal five times in each of the indicated positions. At the end of these passages, they repeat this process with the other three tags, the last being the tag exclusively developed to perform this work. The tag to present the best overall performance is then used for the portal configuration. The evaluation of different tags in the same scenario is to analyze if the proposed tag presents a performance superior to commercial tags that were developed for applications with strong presence of water.

Figure 24 - Portal suggested by (OBERLI, 2010)
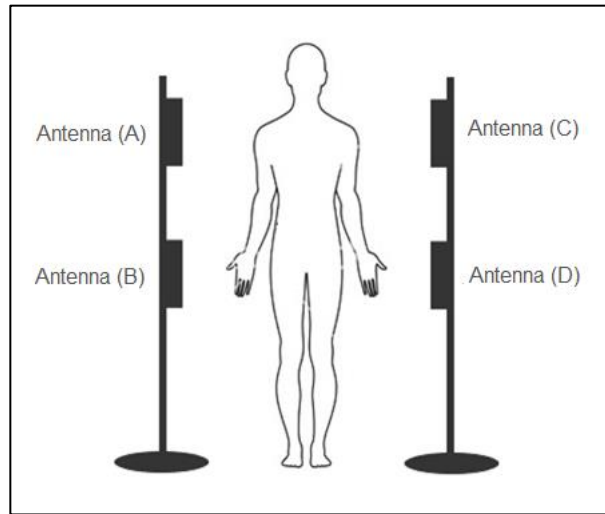
Source: Prepared by the author, 2019.

Figure 25 - Portal top vision
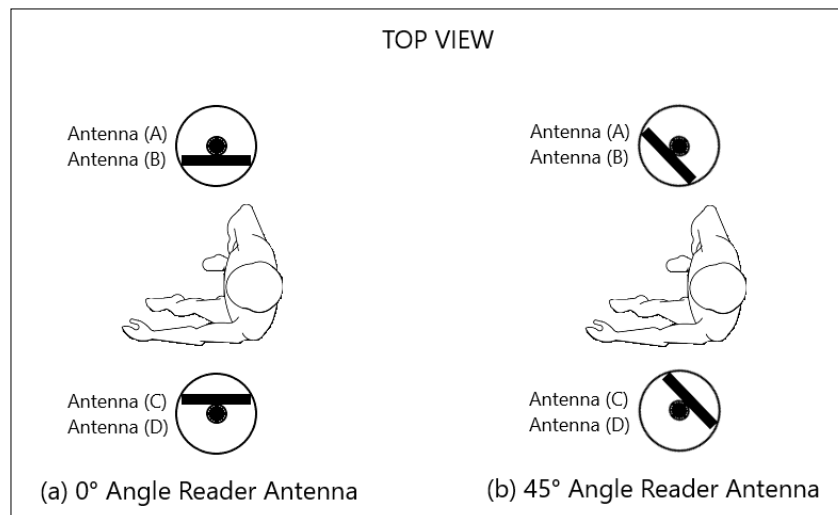
Source: Prepared by the author, 2019.

The volunteers returned once more to execute the process of passing through the portal with all tag carrying positions, but now with adjusted number and height of the reader antennas to obtain the highest tag detection result. In addition to the reference point presented in (OBERLI, 2010) two new heights are evaluated for antenna lines. The first proposal is to lower the bottom line to 50 cm in order to improve the recognition of the tags carried in the socks and the second is to lower the top line to 100 cm in order to increase the waistline coverage region.

The intention of evaluating the application of a smaller number of reader antennas is to optimize the final solution.

After setting the best performance at 0° angle, antennas directed to the opposite side of the portal, the antennas are set to find the angle that allows the largest number of tag reads, Figure 25b. Adjusting the angle of the antennas in order to capture the entrance and exit of the passenger in the portal can lead to an improvement in the recognition of the tag.

Other antenna positions are not evaluated in this thesis because they present greater losses in tag recognition, such as positioning antennas in the upper part of the portal directed downwards.

Using the tag with better performance and configured portal according to the above tests, ten volunteers of different biotypes pass through the portal five times with each of the positions described in Table 3. The results obtained in the individual passage and in pairs (two volunteers passing through the portal side by side), will make possible to evaluate the actual performance of the proposed system and point out the possible future improvements. With these tests, a confidence level of 95% is expected.

One way to assess if the scanning system is detecting the presence of the RFID tag is analyzing the Received Signal Strength Indication (RSSI) level informed by the reader device. Considering that this value obtained is a measure of relative quality related to the power present in a received radio signal, the result of the experiment can represent the influences of the controllable factors in the tag recognition.

The controllable factors considered in this work are the carrying scenarios of the RFID tag present in the passenger card and the biotype of the passenger. Non-controllable factors such as ambient temperature, the way to pass through the portal, thickness and type of clothing material are not considered although they may directly influence in the results presented.

5   ANTENNA PROTOTYPE DEVELOPMENT

According to (GOES, 2014), in order to idealize mathematical modelling, it is necessary to know the RFID system in depth. The Figure 26a, illustrates the system detailed herein. A reader module is connected to four antennas that will form the identification portal. These antennas in turn generate an electromagnetic field of reading which is always active in order to detect some tag. The moment a tag enters this field, an electromagnetic response is induced that will serve as tag identification. As the system proposed here gives freedom for the user to load the tag in several positions, it is necessary to extend the electromagnetic field of reading, so four antennas are used forming a portal. The four antennas emit identical fields, so the read response is the same regardless of which antenna captures the tag.

Figure 26 - RFID System schematic proposal

(a) Illustration of RFID System   (b) Equivalent Circuit of RFID Tag
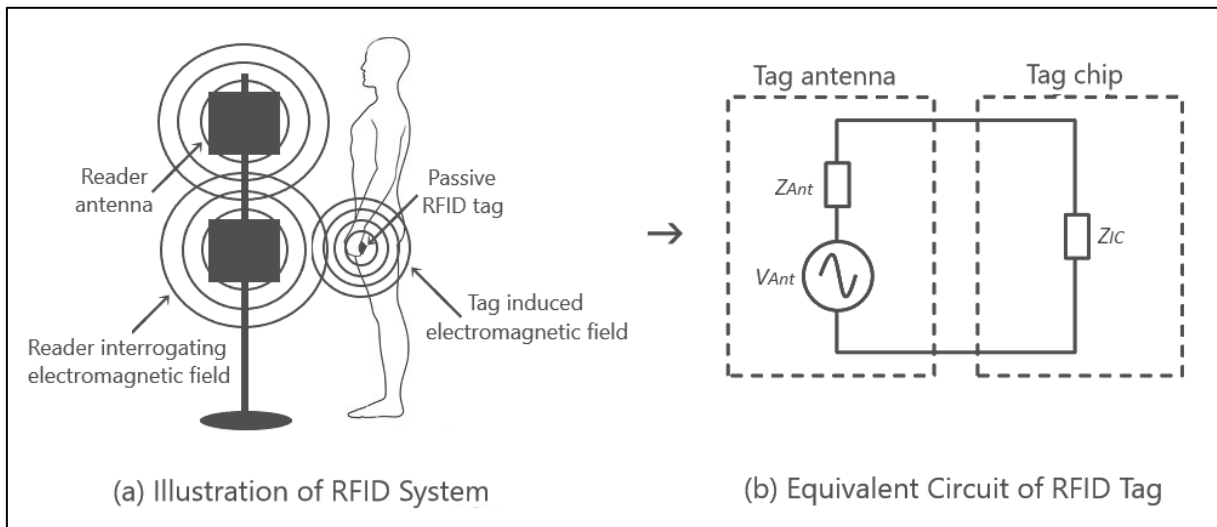
Source: Prepared by the author, 2019.

The RFID tags consist primarily of an antenna and an integrated circuit with complex input impedances (DOBKIN, 2013), as shown in Figure 26b. The integrated circuits are usually located on the antenna connectors and operate under voltage V_{Ant}, received by the external field antenna excited by the reader. To trigger the circuit, it is necessary to guarantee a minimum of energy P_{th} over the required frequency range.

The antenna design is one of the most critical point in passive UHF RFID systems (DOBKIN, 2013). As described in the theoretical basis the antenna transfers the radiated power from the reader antenna to the IC. In order to achieve the maximum power transfer, the antenna impedance (Z_{Ant}) must be the complex conjugate of the IC impedance (Z_{IC}):

$$Z_{Ant} = Z_{IC}^* \tag{37}$$

The antenna is directly connected to the chip, which typically presents a high-capacitive input impedance. The mechanical process of direct attaching the IC to the antenna introduces further parasitic capacitance between the IC and the antenna. The parasitic capacitance due to the assembling process are ideally in parallel to the IC, therefore they are added to the IC capacitance (in case of equivalent parallel model of the IC), Figure 27.

Figure 27 - Equivalent circuit of the IC including parasitic
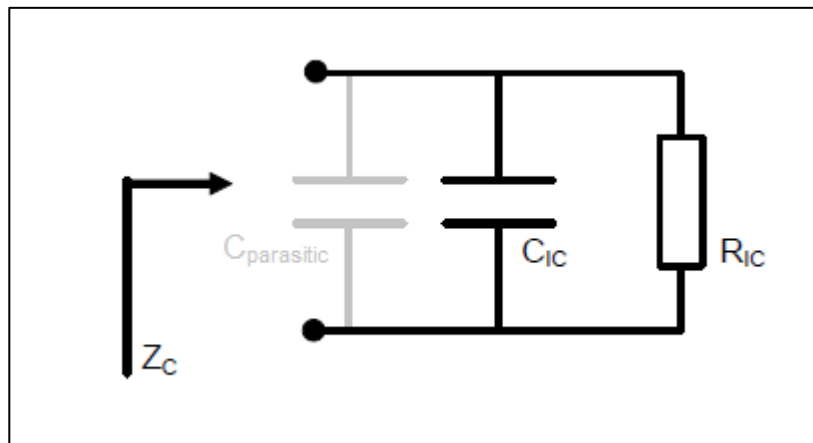
Source: Prepared by the author, 2019.

By taking into account the parasitic effects of the mechanical assembly process, the new impedance of the assembled IC (calculated and or measured) is denoted as Z_C.

To achieve the best matching between the antenna and the IC the following equation must be satisfied.

$$Z_{Ant} = Z_C^* \tag{38}$$

According (BALANIS, 2005), due to physical restriction the exact matching most of time in real life application cannot be achieved.

A way to obtain the best matching between the antenna and the IC is to minimize the power reflection coefficient $|s|^2$ in the following equation:

$$|s|^2 = \left|\frac{Z_{Ant}-Z_C^*}{Z_{Ant}+Z_C}\right|^2 \tag{39}$$

By knowing the tag antenna parameter, it is possible to calculate the RFID tag performance by following:

$$Range = \frac{\lambda}{4\pi}\sqrt{\frac{P_{eirp}G_r}{P_{th}}p(1-|s|^2)} \tag{40}$$

Where λ is the wavelength, P_{eirp} is the equivalent isotropic radiated power transmitted by the reader, Gr is the tag antenna gain, P_{th} is the minimum power required to activate the chip (as provided in the datasheet), and p is the polarization loss factor.

Due to the fact that the antenna shall perform optimal in passenger recognition application (distance between reader and tag antenna > 1m), the antenna design shall be able to receive energy from the radiated electric field. The electric component is the dominant part of the radiated electromagnetic wave in the far field (BALANIS, 2005).

In the far field condition the ratio between the E and H is equal to wave impedance Z_0.

$$Z_0 = \frac{E}{H} \tag{41}$$

$$Z_0 = \sqrt{\frac{\mu_0}{\varepsilon_0}} = 377\Omega \tag{42}$$

Derived from this equation the E field is the dominant part of the radiated wave in far field condition.

The propagation path loss and antenna gain play a crucial role regarding the system performance (BALANIS, 2005). Taking into account these environmental influences, he

antenna design shall be able to power up the IC at distances higher than 1 meter from the reader antenna.

To fulfill the requirements of a far field design (strong E field behavior) this work will focus on a dipole type based antenna. A dipole is able to get maximum coupling with the radiated E-Field and hence harvest most energy from the field. Using a loop as a matching network the dipole is then matched to the IC.

The use of a matching network is necessary due to the fact that a dipole based antenna is mainly a capacitive resonant circuit and the IC with is a capacitive load need to be compensated to match the dipole antenna and satisfy the equation 38.

In it case a capacitive IC impedance (with a negative imaginary part) should be compensated. This refers to the model depicted in Figure 27.

The two parallel capacitances and the parallel resistance that an equivalent impedance in the following form:

$$Z_C = X - jY \tag{43}$$

With both X and Y > 0

A positive imaginary part will be required, in order to get a matched system. The conjugate complex of a capacitive impedance is an inductive impedance (positive imaginary part).

Thus, the antenna will be based on a loop matching network coupled with a dipole.

The loop dimension is influencing the absolute value of the imaginary part of the impedance. The impedance value of the loop shall match as exact as possible the impedance of the IC, regarding the imaginary part as well as the real part.

The positive imaginary part of the loop impedance increases the inductance of the loop (size). The resistance is increased by reducing the width of the trace but this will also influence the bandwidth of the antenna.

The resonance frequency of the dipole is defined by setting the length of the dipole.

The loop based part of the antenna can be schematized as described in Figure 28. The real part of the impedance of the loop consist of a part given by the radiation resistance (Radiation) and a part given by the losses given by the loop conductor (R loss). In general for a small circular loop the radiation resistance is given by the following equation 44.

$$R_{loop,radiation} = 20\pi^2 \frac{c^4}{\lambda^4} \tag{44}$$

The equation shows clearly that the impedance (real part) is strictly related to the area of the loop.

The first limit to the design (based on a matching loop) is given by the chip impedance.

In this work it will be matched to the impedance of the UCODE 7. It requires a loop having a big area to compensate the real part and to generate the necessary inductance to compensate the imaginary part of the chip impedance (NXP, 2017).

The inductance of a small loop is given (approximately) by the equation 45. Where a denotes the loop radius and b the wire radius (with the assumption that the loop is a wire).

Main purpose of equation 45 is to show the dependence of the inductance from the loop dimension.

$$L_A = \mu_0 a \left[\ln \left(\frac{8a}{b} \right) - 2 \right] \tag{45}$$

$$L_i = \frac{l}{\omega P} \sqrt{\frac{\omega \mu_0}{2\sigma}}$$

The second limit is the bandwidth. In this case the chip is an electrical system with a low Q (Q<7). This will lead a broad band loop. Narrowband loops can reduce the performance of the system by limiting the whole bandwidth (DOBKIN, 2013).

Figure 28 - Electrical scheme of a loop antenna
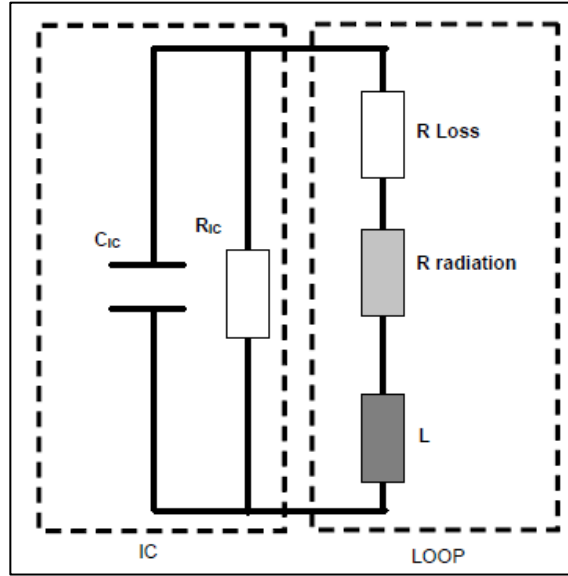
Source: Prepared by the author, 2019.

The typical representation of a dipole is given by a series-L-C resonant circuit showed in Figure 29.

The resonance frequency of the dipole is function of the inductance and capacitance.

For a series L-C resonant structure the resonance frequency is given by the equation 46.

$$\omega_{res} = \frac{1}{\sqrt{LC}} \tag{46}$$

The quality factor and the bandwidth of the dipole as described in Figure 29 are functions of $\sqrt{L/C}$ and of $1/Q$ respectively.

Figure 29 - Electrical scheme of a dipole antenna
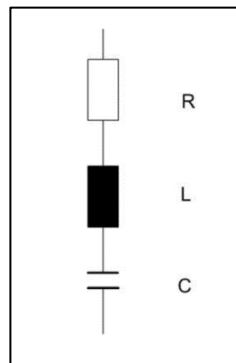
Source: Prepared by the author, 2019.

6 SYSTEM DEPLOYMENT

In order to obtain the advantages already mentioned in the previous chapters it is being decided to elaborate a hybrid system, using devices already present in the market allied to the proposal of a new tag that allows a better adaptation to the application. This chapter discusses the deployment of the system, defining the portal devices and the tag options to be evaluated.

6.1 READER'S SET

The reader set consisting of module and antennas is as important as the tag to ensure the effectiveness of the proposed solution, but there are market options of excellent performance, so the development of such devices was not the focus of this thesis.

6.1.1 Reader Module

The reader module chosen was the Mercure6e (M6e) from ThingMagic, Figure 30. According to (THINGMAGIC, 2013), the M6e can transmit up to +31.5 dBm RF power and has the capacity to read more than 750 tags / seconds, an excellent option considering a mass passenger boarding. With USB and serial communication, it is easy to implement in embedded systems. It can work with up to 4 antennas, allowing a complete management of the portal idealized in this work. The M6e is compatible with various UHF RFID tags, including EPCglobal Gen 2 (ISO 180006C).

Figure 30 - ThinkMagic UHF RFID reader module

Source: Digi-Key website[1].

6.1.2 Reader Antenna

Passive RFID reader antennas are generally physically similar, so it is important to analyze the technical specifications, as this is what differentiates them from each other. To select an RFID reader antenna, the three most important specifications to consider are frequency range, gain / beamwidth and polarization (GOES, 2014).

A. Frequency Range

Each country has regulations that specify the frequency bands for UHF RFID transmissions in that country. In Brazil, Brazilian National Telecommunications Agency (ANATEL) regulates these frequencies, with two bands 902-907 MHz and 915- 928 MHz being released.

B. Gain/Beamwidth

According (BALANIS, 2005), gain and beamwidth are electrical components of an antenna and are clearly related, so in this work this is considered grouped. The higher the gain, the narrower (or lower) the beamwidth. A higher gain creates a narrower coverage area, but the beam will travel a greater distance, as shown in Figure 31.

[1] Available at: <https://www.digikey.com/product-detail/en/thingmagic-a-jadak-brand/M6E/1523-1002-ND/4842686>. Access in: 5 Aug. 2018.

Figure 31 - Relation between gain and beamwidth
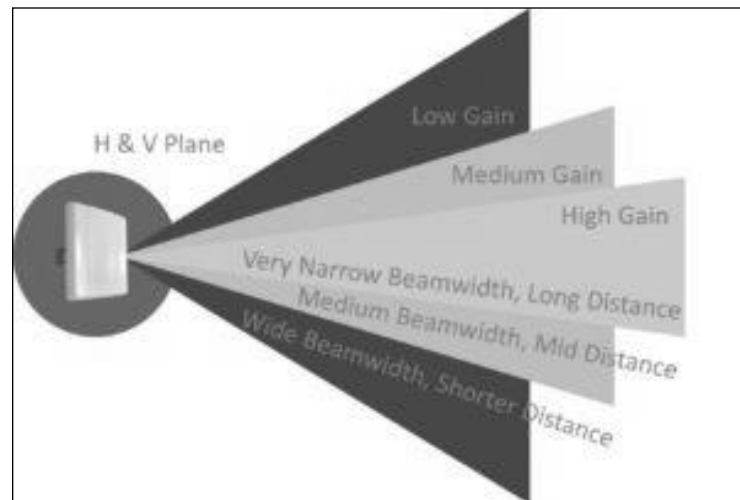
Source: AccelTex website[1].

In this work the optimum beamwidth and gain will depend on the reading distance of the tags. Since many tags may be in the field of reading within a short distance (<1 meter), it doesn't need a high gain antenna. In this case it is more advantageous to use a wide beamwidth antenna with relatively low gain.

C. Polarization

As explained in the theoretical basis, passive UHF RFID antennas have either linear or circular polarization. Linearly polarized antennas send RF waves in a single plane, horizontal or vertical. Circularly polarized antennas send RF waves in circular motions clockwise or counterclockwise. When the waves rotate clockwise, the antenna is circularly polarized to the left; when the waves rotate counterclockwise, the antenna is circularly polarized to the right, Figure 32.

---

[1] Available at: <http://www.acceltex.com/planes-gains-and-beamwidths-reading-radiation-patterns/>. Access in: 5 Aug. 2018.

Figure 32 - Antenna polarization
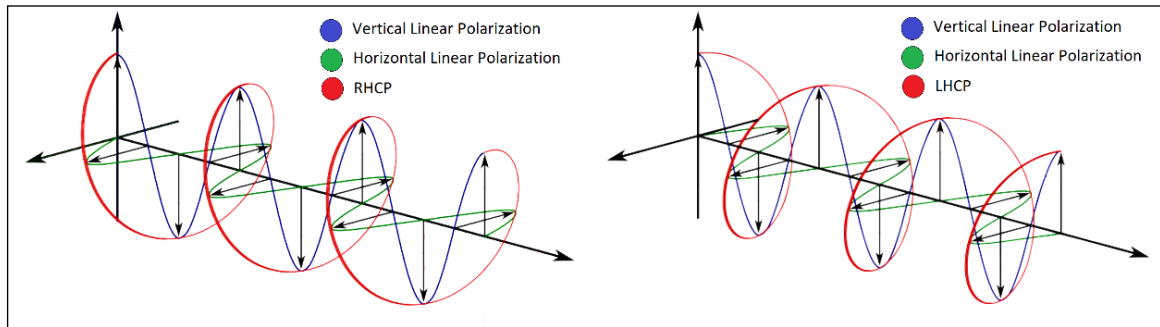
Source: Wikipedia website but modified by the author, 2019[1].

According (DOBKIN, 2013), linearly polarized antennas are ideal in applications where all tags are read with the same orientation and at the same height. When it is not possible to predict the positioning or orientation of the tags the best choice is to use circularly polarized antennas, so it is the option selected for this work.

In a configuration where the antennas are facing each other, it is important to know if you have Left Hand Circular Polarization (LHCP) or Right Hand Circular Polarization (RHCP) antennas. When antennas face and emit waves in the same direction, null zones can occur where the waves overlap, but in a single reader system, which is the situation of this work, this problem does not occur because the RFID reader only activates an antenna at a time.

Taking into consideration the proposed application and the three most important specifications of a static RFID UHF reader antenna, for this work the model 100.098 of Acura was chosen (ACURA, 2016). This model has a frequency range of 902 to 928 MHz, gain of 6 dBi, beam width of 77 ° (horizontal) and 72 ° (vertical) and works in the circular polarization LHCP. The radiation pattern can be seen in Figure 33.

---

[1] Available at: <https://en.wikipedia.org/wiki/Circular_polarization>. Access in: 11 Aug. 2018.

Figure 33 - Radiation diagram
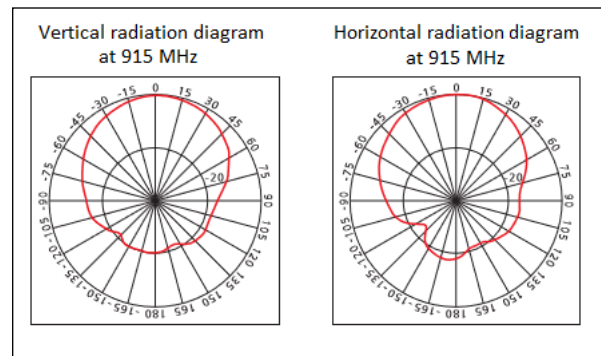
Source: ACURA, 2016.

6.2 PROTOTYPE TAG

To meet the demand to be a RFID tag with a strong presence of water in its vicinity, an antenna was designed that could lessen this scenario. Using the equations presented in both theoretical and mathematical modeling, as well as the CST Microwave Studio (CST, 2010) computer program, an antenna option with central frequency at 890 MHz was developed.

According (BALANIS, 2005), for every tag antenna it has to consider fixed parameters that can't be changed and variable parameters which can be influenced and tuned to meet the requirements of the design. In this context, the design started by specifying the fixed parameters such as Q value, Impedance, and power consumption which are considered as given and constant.

Details like antenna material and required performance of the antenna design are vital inputs for designing an antenna (BALANIS, 2005). Also, in this context, the following design constants were fixed:

- Quality factor Q = 9

- Impedance Z = 22 – j195Ω

- Minimum operating power supply Pmin = -15 dBm

The material that are made up of the existing passenger cards in the market is Polyethylene Terephthalate (PET), so this is the material defined to couple the developed antenna. PET has a dielectric constant of 3.5.

The main aspect of the system based on a loop and a dipole antenna is how to couple two radiating structures (DOBKIN, 2013). In the developed design the loop and the dipole are connected using conducted coupling.

The Figure 34 shows the design of the label with quotes. The dipole part of the antenna and the loop area are depicted.

Figure 34 - Antenna dipole and loop area
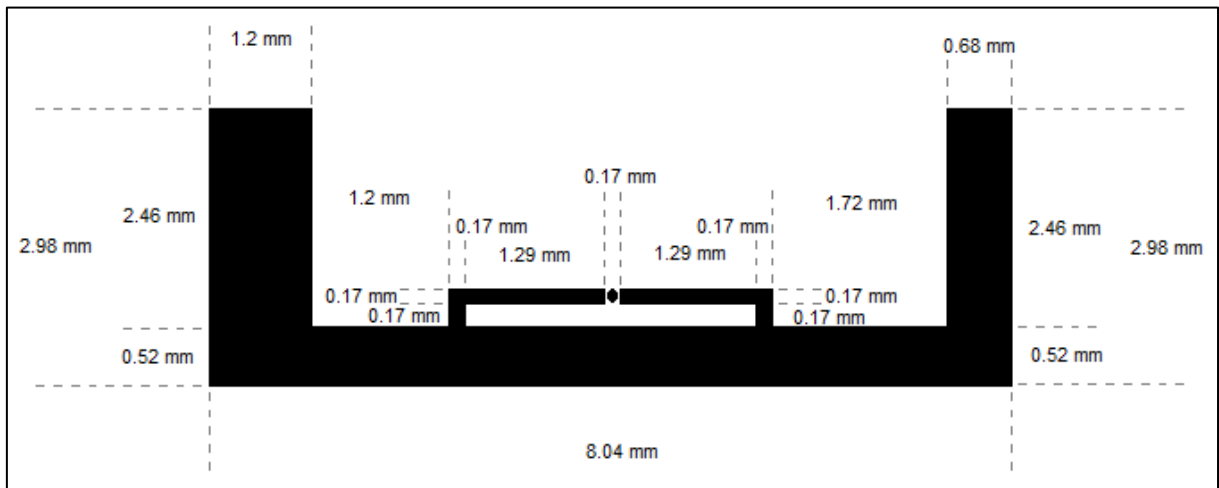
Source: Prepared by the author, 2019.

As the initial proposal is not to replace the current passenger card, since MIFARE technology has security encryption, something extremely important for the validation issue, the developed tag is coupled to the existing card, making the hybrid card with two technologies RFID, the HF for validation and the UHF for recognition, according to Figure 35.

Figure 35 - Proposed passenger final card
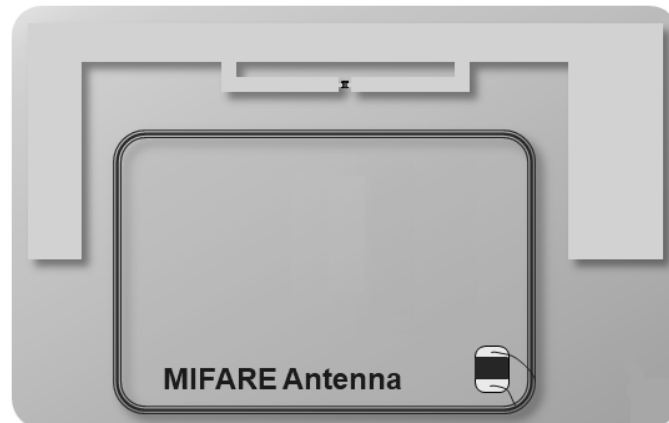
Source: Prepared by the author, 2019.

6.3 OTHER TAGS

The purpose of this thesis is not only to elaborate a passive tag with good performance to be used close to the human body, but also to evaluate market tags that have feasibility to be used in this application. Following this context, three passive market tags were selected: AD-370u7, RSI-650 and RSI-654.

6.1.1 AD-370u7

Developed and supplied by Avery Dennison is a general purpose supply chain tag, Figure 36. With operating frequency of 860 to 960 MHz and use of the NXP UCODE 7 chip, which works with the EPC Gen 2 Class I protocol (DENNISON, 2018), this tag is prepared to be recognized by the portal idealized in this thesis.

Figure 36 - Avery Dennison AD-370u7 tag
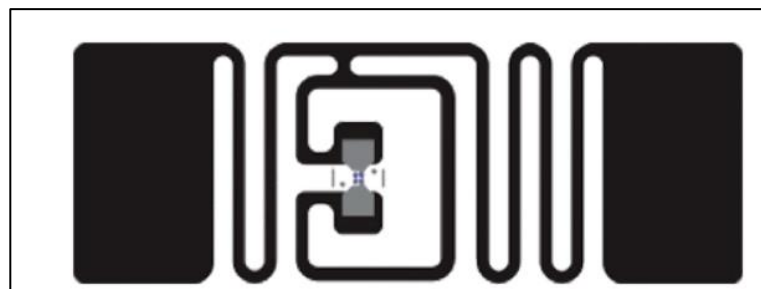
Source: DENNISON, 2018.

6.1.2 RSI-650

The RSI-650 from Sirit is a medium-sized, high-performance tag designed for use in applications with size limitations and works best when applied to plastic, Figure 37. Designed for use with NXP UCODE chips, it works from 865 at 928 MHz (SIRIT, 2016a).

Figure 37 - Sirit RSI-650 tag
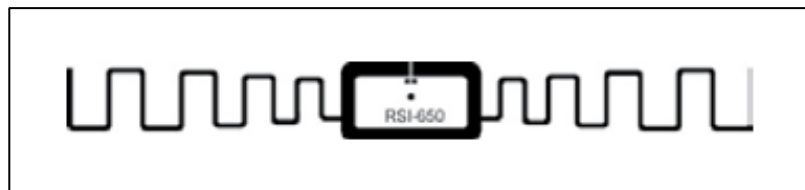
Source: SIRIT, 2016.

6.1.3 RSI-654

The RSI-654 design offers high performance in plastic, cardboard and water based products, making it ideal for commonly used applications, Figure 38. Like the other tags here, it uses the NXP UCODE chip and works in the frequency of 865 to 928 MHz (SIRIT, 2016b).

Figure 38 - Sirit RSI-654 tag

Source: SIRIT, 2016.

7 VERIFICATION AND VALIDATION

7.1 SURVEY

In the (OBERLI, 2010) study the following card portability scenarios were analyzed:

- In the hand

- In the wallet in the backpack

- In the wallet in the pants' right back pocket

- Loose in the pants' right back pocket.

The author considered these four scenarios as the most common to carry an identification card, which may be valid as proof of concept, but for evaluation of the applicability of technology in public transport becomes a poor analysis. As a result, it was decided to carry out an informal survey with a group of users of public urban transport to map the most varied forms of card portability.

The focus of the research was the users of line D43, University - Direct, between March 8 and 9, 2016. For each passenger, at the moment they were waiting for the arrival of the bus in the terminal Campus of Agronomy, the following question was asked: Are you a constant user of public transportation? If the answer was yes, the last question was asked: How do you carry the pass validation card?

In all, 120 users were interviewed and the results of the research can be seen in Table 2.

Table 2 - Informal search result with 120 public transport users

Answers for second question	Number of related users
Inside the wallet in the back right pocket of pants	32
In the wallet inside the backpack/briefcase	26
In the front pocket of pants	19
In the back pocket of pants	17
In the backpack/briefcase	14
On the hand	6
In the shirt pocket	5
In the sock	1

Source: Prepared by the author, 2019.

Based on the research results, 14 forms of card portability were defined which are used to evaluate the performance of the system, Table 3 and Figure 39.

Table 3 - Tag carrying positions

Reference	Description
1	On the left hand
2	In the front left pocket of pants
3	In the front right pocket of pants
4	In the right sock
5	In the shirt pocket
6	In the left sock
7	On the right hand
8	In the right front pocket of pants along with keys
9	In the right front pocket of pants along with the cell phone
10	In the back right pocket of pants
11	In the back left pocket of pants
12	Inside the wallet in the back right pocket of pants
13	In the backpack
14	In the wallet inside the backpack

Source: Prepared by the author, 2019.

Figure 39 - Front and rear view of the volunteer in the portal
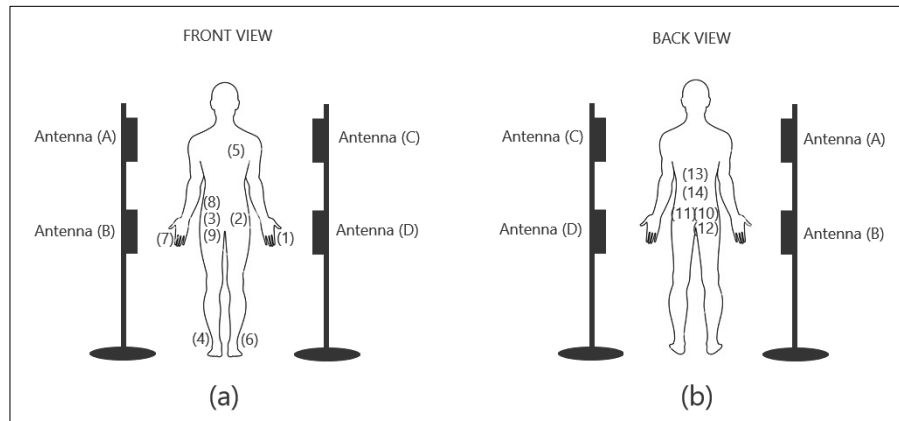
Source: Prepared by the author, 2019.

7.2 EXPERIMENTS

A schedule of 140 measurements was defined, to ensure that a random process was done. In Table 4 is possible verify the order of the measurements. Also, is possible verify that in this point was assumed that the experiment is composed by two controllable factors: the volunteers, with two levels of control and the tag carrying position, with fourteen levels of control. In order to apply the analysis algorithm, the volunteers are considered Factor A and the tag carrying position like Factor B. Both factors and its levels are also identified in Table 4.

To assist in the analysis of the applied model, Minitab 17 statistical software is used.

As described in (TASHI, 2011; TSAI, 2012), the definition of the tag is extremely important for the result to be as close to the expected one. Following this concept, the first action was to find the tag with the best performance. The experiments were performed using the reader system installed as shown in Figure 40a, outlining the constructed prototype, which is shown in Figure 40b. The power used was 10 dBm (4 dBm + 6 dBi), because it is necessary to use a wide beamwidth. Two volunteers passed through the portal five times with each of the possible tag carrying positions according Table 4. This test was performed with each of the four tag options, three commercial and one designed.

Table 4 - Schedule of 140 measurements

| Ref. | Volunteer A | | | | | Volunteer B | | | | |
Table 3	S1	S2	S3	S4	S5	S1	S2	S3	S4	S5
1	1	39	57	85	125	4	34	64	90	128
2	9	49	67	107	123	14	52	62	100	122
3	17	53	63	89	139	2	44	80	112	114
4	15	35	75	99	129	18	32	58	92	134
5	3	55	79	111	131	6	54	78	98	124
6	11	29	81	93	137	24	36	70	106	118
7	21	41	73	87	113	10	50	66	108	130
8	5	45	59	105	117	12	30	72	96	120
9	7	47	65	91	127	16	48	76	102	138
10	23	37	77	97	121	22	40	82	86	126
11	19	31	69	101	133	8	42	60	94	116
12	25	43	61	109	119	20	38	68	104	140
13	27	51	83	95	115	28	56	84	110	136
14	13	33	71	103	135	26	46	74	88	132

Source: Prepared by the author, 2019.

Figure 40 - The portal prototype
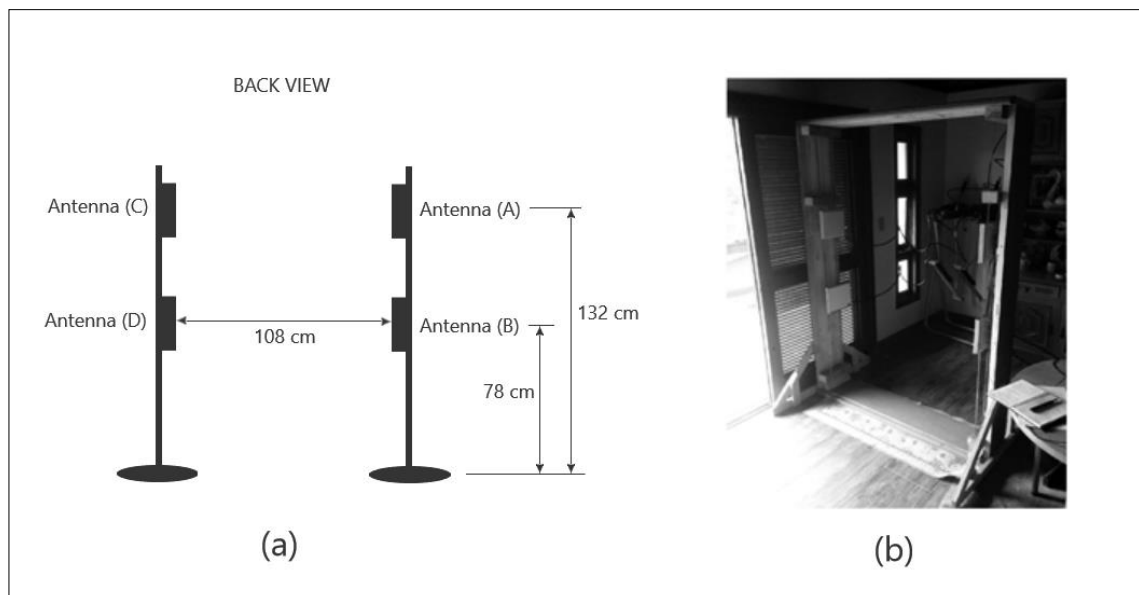
Source: Prepared by the author, 2019.

The next step was to define the height of the antenna lines. Beyond the reference point presented in (OBERLI, 2010), it was assessed 50 cm on the bottom line and 100 cm on the top line. The analysis process was the same performed in the tag test.

With height and tag adjusted, the angular position of the readers' antennas was evaluated. Initially the antenna A was adjusted to 45° tilt and the antenna C to - 45°, leaving antennas B and D in the original position. After the tests with two volunteers, it was changed the position of the antennas B and D leaving - 45° and 45° respectively. The tag carrying tests were run again and in the end, the antennas A and C were returned to the original position to another test set.

The final step adjustments using only two volunteers was the evaluation of performance with less than 4 antennas. The intention of this test was to raise the gain that each antenna gives the system. Initially only the antenna C has been enabled, then only the antenna D, soon after the antenna B has been enabled, and finally the antenna C. With each antenna was evaluated the tag carrying to raise all the response curves.

Some statistical analyzes were performed on the data obtained to evaluate if the controllable factors considered in this thesis influence the results. The tool used in this study was the Analysis of Variance (ANOVA).

In order to prove the actual performance of the selected tag in the practical test for the proposed application, it was carried out an assessment in a controlled environment before the collective test. In this environment it is assessed some of the positions listed in Table 3, using laboratory equipment.

After the lab test, with the portal configured to obtain the best reading and with the selected tag, it was performed more tests with ten volunteers from different biotypes. According to (BOX, 2005), as more samples of different profiles, better the data reliability will be. Each

user received a similar tag and they crossed the portal five times with each one of the fourteen tag carrying options described in Table 3.

7.3 RESULTS

The first stage of tests was performed in order to configure the portal to set the tag to the collective test. This phase was carried out with two volunteers of different biotypes. Volunteer A measuring 178 cm tall and weighing 125 kg, the fact that he is a person with a high body mass index tends to be an important factor in the analysis of the system since the human body, as has been mentioned above, interferes in the tag reading as it is majorly constituted of water. Volunteer B with 188 cm tall and 93 kg had a lower Body Mass Index (BMI), promoting a comparative analysis of the system between two people of different biotypes.

The first evaluation proposal was to analyze, in a group of four distinct tags (Figure 41), which was the most appropriate tag for the application as electronic ticketing card, considering that it will not be exposed directly to a reader. According to the results presented in Table 5, with the "c" tag from a total of 140 passes, it was recognized 99 times, accounting for 70.71% efficacy. The tags "a", "b" and "d" in a general context are inferior in accuracy, presenting 55.71%, 61.43% and 69.29% respectively. Since the difference between the tag "c" and "d" was less than 2%, it will be reassessed performance of these two tags after the final configuration of the portal.

Figure 41 - RFID tags evaluated: a) Avery Dennison AD-370u7; b) Sirit RSI-650; c) Sirit RSI-654; d) Prototype
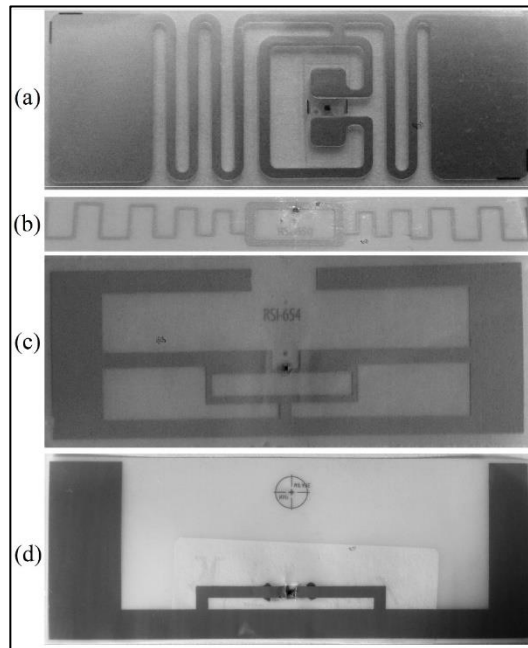
Source: Prepared by the author, 2019.

After completion of the first analysis, the study was aimed at assessing the portal. Following the study performed by (OBERLI, 2010), it was evaluated how a change in the height, in the angle and in the number of antennas could affect the system performance.

Four antennas height settings were used having the best configuration with antennas A and C at 100 cm from the ground and B and D antennas at 78 cm, see Figure 42 and Table 6. This distribution increased the performance at 7.14% compared to that suggested in (OBERLI, 2010). There were 109 recognitions within a scenario of 140 passes through the portal.

Table 5 - Results for tag model C in the first analysis

Ref.	Volunteer A					Volunteer B				
Table 3	S1	S2	S3	S4	S5	S6	S7	S8	S9	S10
1	X	X	X	X	X	X	X	X	X	X
2	X	X	X	X	X	0	0	0	X	X
3	X	X	X	X	X	X	X	X	X	X
4	0	0	0	0	0	0	0	0	0	0
5	X	X	X	0	X	X	X	X	X	X
6	0	0	0	0	0	0	0	0	0	0
7	X	X	X	X	X	X	0	X	X	X
8	X	X	X	X	X	X	X	X	X	X
9	X	X	X	0	0	X	0	0	0	0
10	X	X	X	X	X	X	X	X	X	X
11	X	X	X	X	X	0	0	0	0	0
12	X	X	X	X	X	0	0	0	0	0
13	X	X	X	X	X	X	X	X	X	X
14	X	X	X	X	X	X	X	X	X	X

TAG ANALYSIS

X – Recognized card

0 – Unrecognized card

Source: Prepared by the author, 2019.

Figure 42 - The final height of reader antennas
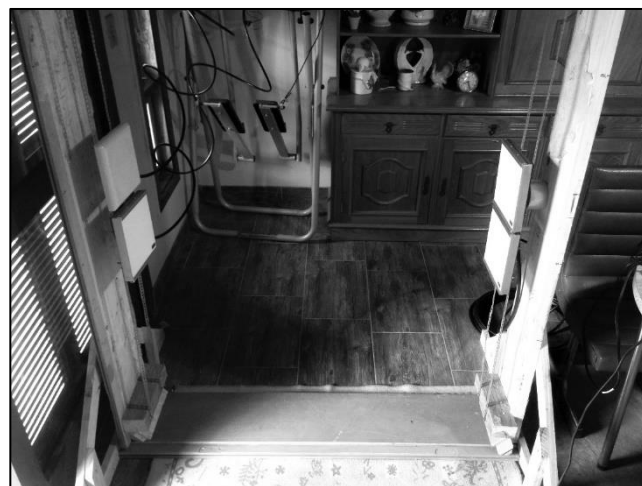
Source: Prepared by the author, 2019.

Table 6 - Results of reader antennas at 100 cm and 78 cm

Ref.	Volunteer A					Volunteer B				
Table 3	S1	S2	S3	S4	S5	S6	S7	S8	S9	S10
1	X	X	X	X	X	X	0	X	X	X
2	X	X	X	X	X	X	X	X	X	X
3	X	X	X	X	X	X	X	X	X	X
4	0	0	0	0	0	0	0	0	0	0
5	0	X	X	0	X	X	X	X	X	X
6	0	0	0	0	0	0	0	0	0	0
7	X	X	X	X	X	X	X	X	X	X
8	X	X	X	X	X	X	X	X	X	X
9	0	X	X	X	0	0	0	0	0	0
10	X	X	X	X	X	X	X	X	X	X
11	0	X	X	X	X	X	X	X	X	X
12	X	X	X	X	X	X	X	X	X	X
13	X	X	X	X	X	X	X	X	X	X
14	X	X	X	X	X	X	X	X	X	X

X – Recognized card

0 – Unrecognized card

Source: Prepared by the author, 2019.

Based on previous result, it was evaluated if the antennas with angulation of 45° could increase the recognition of tags in different carrying positions (Figure 43). The best result was acquired with the antenna A adjusted to 45° tilt and the antenna C to - 45°, leaving antennas B and D in the original position. The results in Table 7 indicate that the change of angle does not represent gains in any forms of tag carrying, but decreased the overall efficacy of the system. It was decreased by at least 0.71%.

Figure 43 - One of the evaluated angular positions of reader's antennas

Source: Prepared by the author, 2019.

Table 7 - Results of reader antennas with 45° angle

Ref.	Volunteer A					Volunteer B				
Table 3	S1	S2	S3	S4	S5	S6	S7	S8	S9	S10
1	X	X	X	X	X	X	X	X	X	X
2	X	X	X	X	X	X	X	X	X	X
3	X	X	X	X	X	X	X	X	X	X
4	0	0	X	0	X	0	0	0	0	0
5	0	0	0	0	0	X	X	X	X	X
6	0	0	X	X	X	0	0	0	0	0
7	X	X	X	X	X	X	X	X	X	X
8	X	X	X	X	X	X	X	X	X	X
9	0	0	0	0	0	0	0	0	0	0
10	X	X	X	X	X	X	X	X	X	X
11	X	X	X	X	X	X	X	X	0	X
12	X	X	X	0	X	X	X	X	X	X
13	X	X	X	X	X	X	X	X	X	X
14	X	X	X	X	X	X	X	X	X	X

X – Recognized card

0 – Unrecognized card

Source: Prepared by the author, 2019.

The last test proposed in the first phase of the work was the analysis of the number of antennas. The reference used in this work signaled that the portal should have four antennas, two per side, and the results presented in Table 8 proved that assertion. With only one enabled antenna, regardless of the side, there was a good reading of the tag, but this only occurred when

the card was not being influenced by the body's voluntary. Hardly the card was detected when it was on the opposite side of the antenna. When two antennas are enabled, one at each side on the bottom line, there was an increase of almost 20% in readings. The third and fourth addition antennas improved the performance, but this improvement was not too high because they focus a body area in which the card is hardly carried.

Table 8 - Results with only D reader antenna

	READER ANTENNA NUMBER ANALYSIS									
Ref.	Volunteer A					Volunteer B				
Table 3	S1	S2	S3	S4	S5	S6	S7	S8	S9	S10
1	X	X	0	X	X	X	X	X	X	X
2	X	0	X	0	0	X	X	X	X	0
3	X	X	X	X	X	X	X	X	X	X
4	0	0	0	0	0	0	0	0	0	0
5	0	0	0	0	0	0	0	0	0	0
6	0	0	0	0	0	0	0	0	0	0
7	X	X	X	X	X	X	X	X	X	X
8	X	X	X	X	X	X	X	X	X	X
9	0	0	0	0	0	0	0	0	0	0
10	X	X	X	X	X	X	X	X	X	X
11	X	0	0	0	X	0	0	0	0	0
12	X	X	X	X	X	X	X	X	X	X
13	X	X	X	X	X	0	0	0	0	0
14	X	X	X	0	X	X	X	X	X	X

X – Recognized card

0 – Unrecognized card

Source: Prepared by the author, 2019.

As already presented, using the tag "c" and applying the best configuration of the portal, the recognition performance was 77.85%. As the initial tag test signaled a small difference between the "c" and "d" tags, the prototype tag was evaluated with the final portal configuration. The data showed a reversal in the results now favoring tag "d", with 80.71% of recognition. One of the evaluated points in this analysis was the received signal strength indication presented by tag every time a volunteer passed by the portal. As mentioned in the last session, a random

schedule of measurements was defined and in Table 9 and Figure 44 is possible verify the results of the RSSI level.

Table 9 - Results of D model tag with the reader antennas at 100 cm and 78 cm with 0° angle

Ref.	Volunteer A					Volunteer B				
Table 3	S1	S2	S3	S4	S5	S1	S2	S3	S4	S5
1	67(1)	70(39)	68(57)	70(85)	71(125)	69(4)	67(34)	72(64)	66(90)	59(128)
2	65(9)	69(49)	64(67)	75(107)	65(123)	65(14)	71(52)	72(62)	62(100)	61(122)
3	70(17)	71(53)	67(63)	69(89)	67(139)	72(2)	67(44)	70(80)	61(112)	71(114)
4	92(15)	92(35)	92(75)	92(99)	92(129)	92(18)	92(32)	92(58)	92(92)	92(134)
5	77(3)	83(55)	80(79)	92(111)	81(131)	71(6)	68(54)	71(78)	71(98)	74(124)
6	92(11)	92(29)	92(81)	92(93)	92(137)	92(24)	92(36)	92(70)	92(106)	92(118)
7	61(21)	63(41)	63(73)	63(87)	68(113)	63(10)	92(50)	67(66)	71(108)	70(130)
8	78(5)	88(45)	82(59)	84(105)	89(117)	73(12)	80(30)	77(72)	70(96)	75(120)
9	89(7)	87(47)	85(65)	92(91)	92(127)	87(16)	92(48)	92(76)	92(102)	92(138)
10	69(23)	65(37)	71(77)	77(97)	72(121)	67(22)	71(40)	57(82)	69(86)	71(126)
11	62(19)	67(31)	67(69)	80(101)	69(133)	89(8)	67(42)	74(60)	61(94)	65(116)
12	55(25)	57(43)	59(61)	55(109)	60(119)	57(20)	59(38)	57(68)	57(104)	60(140)
13	40(27)	41(51)	57(83)	49(95)	42(115)	40(28)	39(56)	44(84)	47(110)	44(136)
14	56(13)	52(33)	61(71)	59(103)	57(135)	63(26)	54(46)	69(74)	67(88)	61(132)

* - All RSSI values are negatives

Source: Prepared by the author, 2019.

Looking only the variation's range of the measurements is difficult to define if the volunteers and the tag carrying positions have influence in the RSSI level and consequently in the tag recognition, so it was necessary to use the ANOVA table to verify if the hypotheses are true. The first step is applying a residual analysis, Table 10 and Figure 45.

Figure 44 - Interval plot of RSSI vs tag carrying position
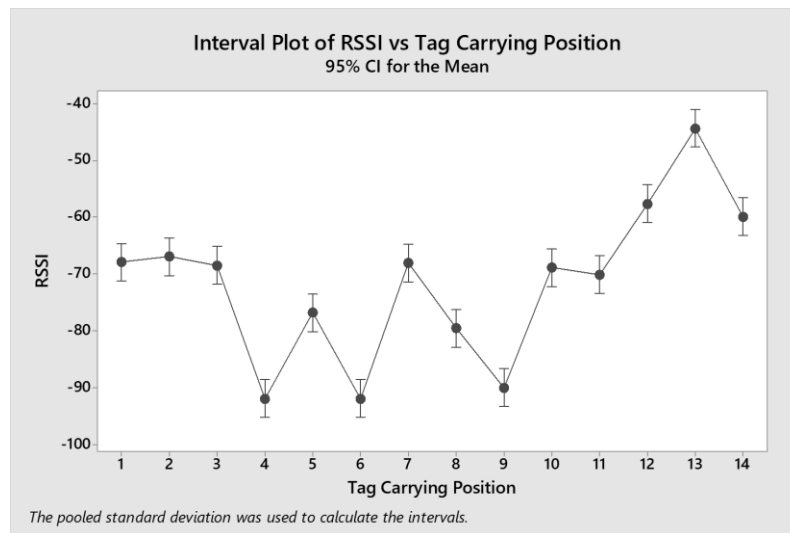
Source: Prepared by the author, 2019.

Table 10 - Residuals

Ref.	Volunteer A					Volunteer B				
Table 3	S1	S2	S3	S4	S5	S1	S2	S3	S4	S5
1	2,2	-0,8	1,2	-0,8	-1,8	-2,4	-0,4	-5,4	0,6	7,6
2	2,6	-1,4	3,6	-7,4	2,6	1,2	-4,8	-5,8	4,2	5,2
3	-1,2	-2,2	1,8	-0,2	1,8	-3,8	1,2	-1,8	7,2	-2,8
4	0,0	0,0	0,0	0,0	0,0	0,0	0,0	0,0	0,0	0,0
5	5,6	-0,4	2,6	-9,4	1,6	0,0	3,0	0,0	0,0	-3,0
6	-0,0	-0,0	-0,0	-0,0	-0,0	-0,0	-0,0	-0,0	-0,0	-0,0
7	2,6	0,6	0,6	0,6	-4,4	9,6	-19,4	5,6	1,6	2,6
8	6,2	-3,8	2,2	0,2	-4,8	2,0	-5,0	-2,0	5,0	0,0
9	0,0	2,0	4,0	-3,0	-3,0	4,0	-1,0	-1,0	-1,0	-1,0
10	1,8	5,8	-0,2	-6,2	-1,2	0,0	-4,0	10,0	-2,0	-4,0
11	7,0	2,0	2,0	-11,0	0,0	-17,8	4,2	-2,8	10,2	6,2
12	2,2	0,2	-1,8	2,2	-2,8	1,0	-1,0	1,0	1,0	-2,0
13	5,8	4,8	-11,2	-3,2	3,8	2,8	3,8	-1,2	-4,2	-1,2
14	1,0	5,0	-4,0	-2,0	0,0	-0,2	8,8	-6,2	-4,2	1,8

Source: Prepared by the author, 2019.

Figure 45 - Residuals vs Order for RSSI
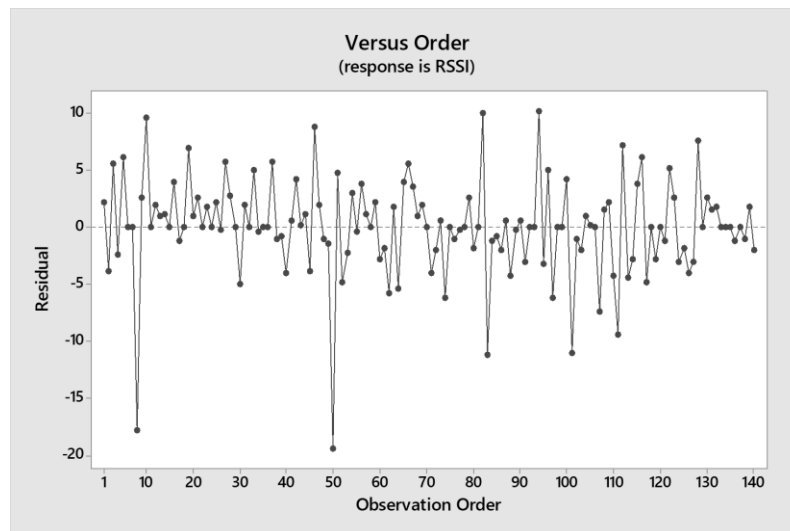
Source: Prepared by the author, 2019.

Analyzing the residuals distribution showed in Figure 45, is possible verify that there is no reason to suspect any violation of the independence or constant variance assumptions once there is no positive correlation between the points in the graphic.

Another possibility of verifying if the design is according the premises is plotting residual versus fits of the treatments. In Figure 46 it is possible to observe that the residuals do not follow any apparent model or structure, being uncorrelated of any other variable.

Figure 46 - Residuals vs Fits for RSSI
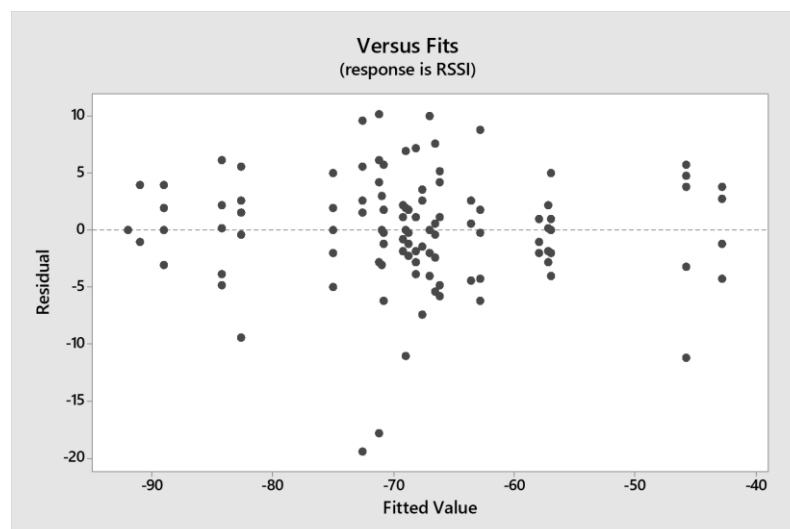
Source: Prepared by the author, 2019.

The residual histogram plotted in Figure 47, shows that the RSSI residual is close the normal distribution. Figure 48 contributes with this understanding, the residual distribution is normally distributed, showing a trend nearly linear. Other information showed in Figure 48 is the normality test using the Ryan-Joiner model. The Ryan-Joiner test with RJ > 0,05 suggests that there is no evidence that the premise of error normality was violated (with a significance level of 0.05).

Figure 47 - Residual histogram for RSSI
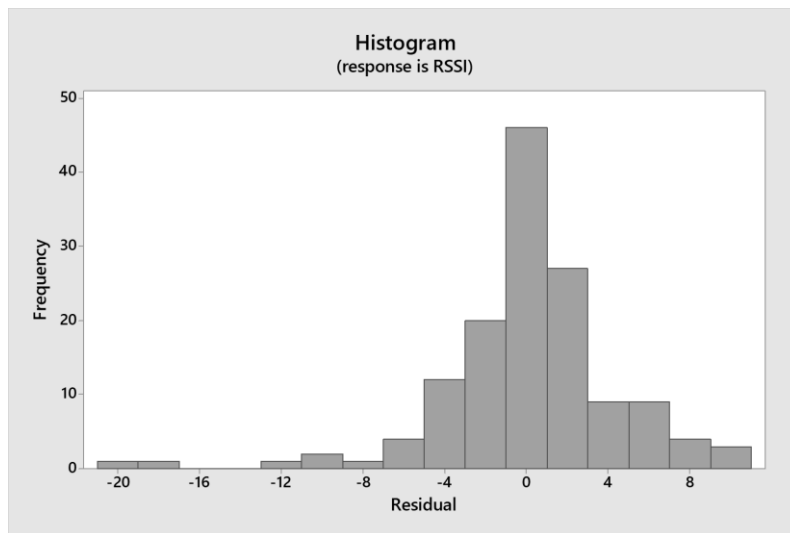
Source: Prepared by the author, 2019.

Figure 48 - Probability plot of residuals for RSSI
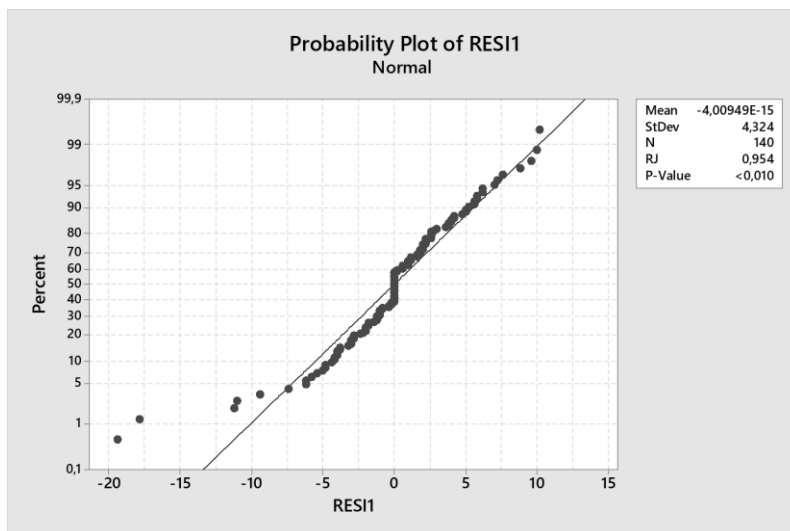
Source: Prepared by the author, 2019.

After being finished the preliminary measurements and after concluding that all requirements of a complete factorial experiment were complied with, was necessary verify if the number of taken measurements was enough to assure a good response of the statistical data. So, the next step was using the Operating Characteristics Curves to determine how many repetitions are necessary for each testing. An Operating Characteristic Curve (Power Curve), according (MONTGOMERY, 2012), is a plot of the type II error probability of a statistical test for a particular sample size versus a parameter that reflects the extent to which the null hypothesis is false. (MONTGOMERY, 2012) also said that these curves can be used to guide the experiment in selecting the number of replicates so that the design will be sensitive to important potential differences in the treatments. Figure 49 shows the power curve for this experiment considering the standard deviation like 4,81, $\alpha = 0.05$, fourteen levels and ten samples.

Figure 49 - Power curve
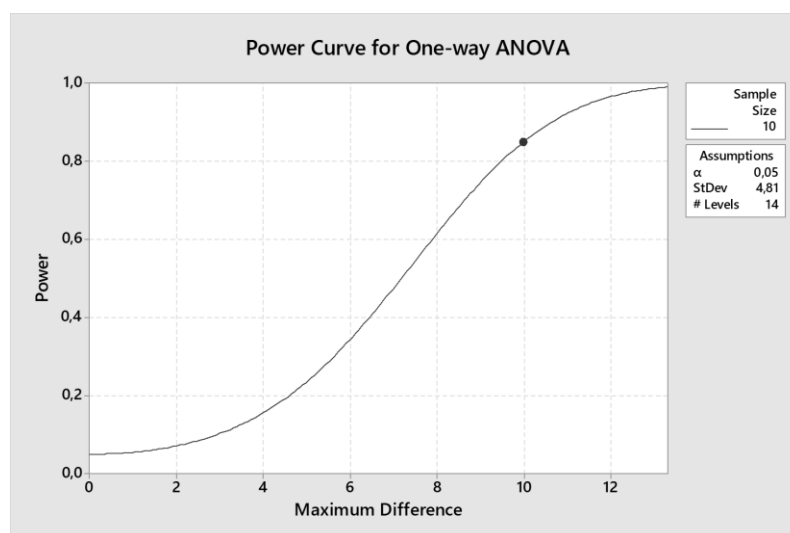
Source: Prepared by the author, 2019.

With ten samples there are more than 80% chance of rejecting the null hypothesis if the maximum difference between means were 9 or more.

Now with the Minitab 17 software is possible to use the ANOVA table to verify if the hypotheses are true, Table 11.

Table 11 - ANOVA table for this experiment based on Minitab 17

		ANOVA			
Source of Variation	Sum of Squares	Degrees of Freedom	Mean Square	$F_{CALCULATED}$	$FT_{0,05;\delta1;\delta2}$
Volunteer (A)	27,5	1	27,46	1,18	3,92
Tag Carrying Position (B)	24072,8	13	1851,75	79,80	1,83
Interaction (AB)	912,1	13	70,16	3,02	1,83
Error	2598,8	112	23,20		
Total	27611,2	139			

Source: Prepared by the author, 2019.

From Table 11 is possible verify that the calculated value of F is greater than the values of F obtained from F distribution of Snedecor ($\propto = 0.05$). This affirmation is true for "B Factor" (tag carrying position) and for "AB Factor" (interaction). In both cases the individual comparison indicates that these factors are significant for the application, so, it is possible conclude that the hypotheses Ho previously declared is false. On the other hand, the A Factor (volunteer) has a calculated F value lower than F tabulated, indicating that the hypothesis Ho previously declared is true.

According (MONTGOMERY, 2012), when the null hypothesis is rejected, it means that there are differences between the treatment means, so in these cases of tag carrying position (B Factor) and the interaction (AB Factor), further comparisons and analysis among groups of treatments means may be useful. Considering this principle as true was elaborated the Table 12 with the means values. Figure 50 graphically shows the means values.

Table 12 - Controllable factors means

	RSSI ANALYSIS		
	Mean A1	Mean A2	Mean B
Mean B1	-69,2	-66,6	-67,90
Mean B2	-67,6	-66,2	-66,90
Mean B3	-68,8	-68,2	-68,50
Mean B4	-92,0	-92,0	-92,00
Mean B5	-82,6	-71,0	-76,80
Mean B6	-92,0	-92,0	-92,00
Mean B7	-63,6	-72,6	-68,10
Mean B8	-84,2	-75,0	-79,60
Mean B9	-89,0	-91,0	-90,00
Mean B10	-70,8	-67,0	-68,90
Mean B11	-69,0	-71,2	-70,10
Mean B12	-57,2	-58,0	-57,60
Mean B13	-45,8	-42,8	-44,30
Mean B14	-57,0	-62,8	-59,90
Mean A	-70,74	-71,55	

Source: Prepared by the author, 2019.

Figure 50 - Main effects plot for RSSI
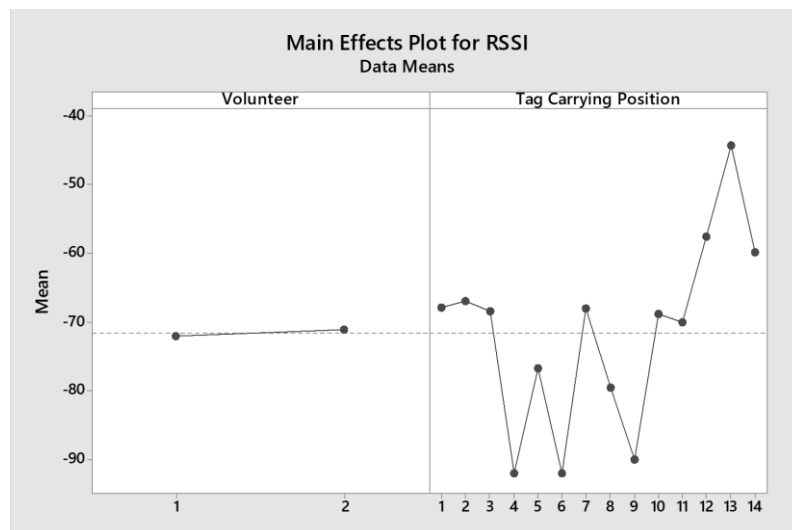
Source: Prepared by the author, 2019.

Analyzing the results of the means it is possible to verify that the volunteers, despite having a very different biotype, have little influence on the means obtained, confirming the ANOVA that this controllable factor is not significant in the variation of RSSI level. On the

other hand, analyzing the means results of tag carrying positions, is possible verify the volunteers who carry the tag in the backpack was the best recognition, while the tag carrying in the socks, independent of the side, was the worst recognition. Another way to carrying with a small recognition is when the user put the cell phone together with the tag. Figure 51 shows the interaction graph, where it is possible observe crossings that proves that the hypothesis Ho is false.

Figure 51 - Interaction plot for RSSI
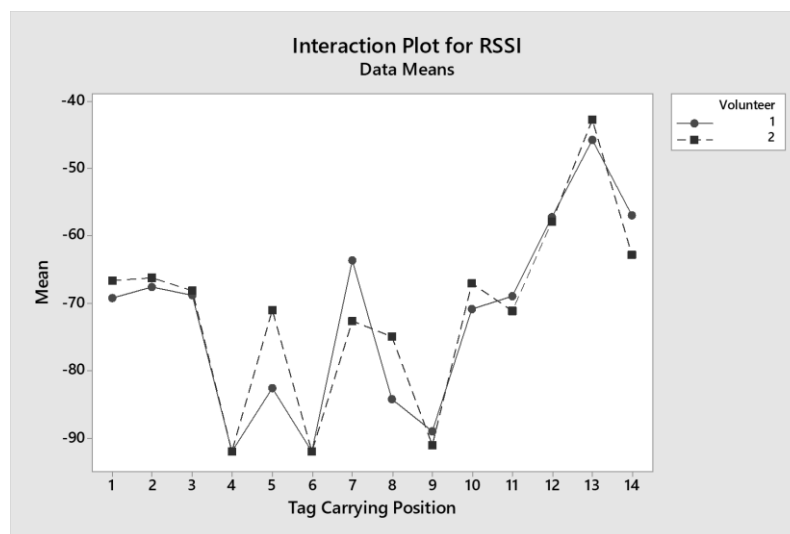
Source: Prepared by the author, 2019.

By rejecting the hypothesis Ho it is possible to conclude that at least 2 levels of the population are significantly different. Using Minitab 17 software it was possible to analyze this aspect and to verify which levels, in the case, which means are different with the use of a technique of multiple comparison of averages, Tukey's Multiple Comparison Method.

In Figure 52 it is possible to observe the multiple comparison intervals for the standard deviation with 95% confidence and in the Table 13 the groups formed. Means that do not share a letter are significantly different.

Figure 52 - Test for equal variances: RSSI vs volunteer; tag carrying position
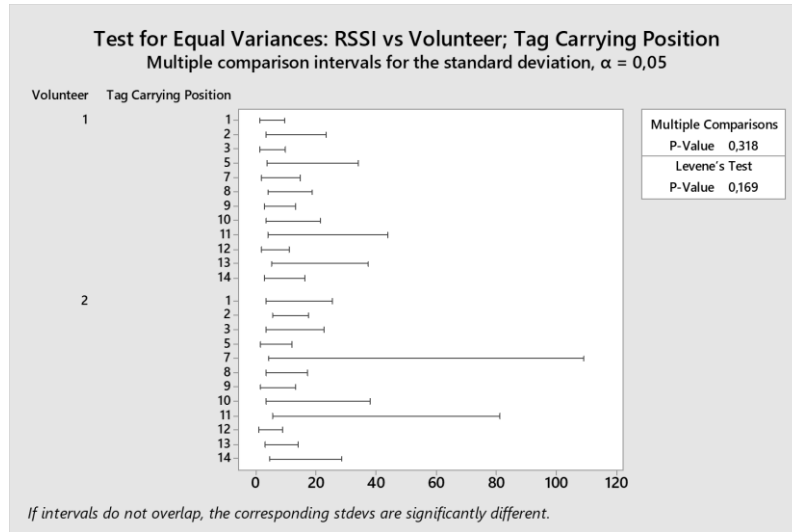
Source: Prepared by the author, 2019.

Table 13 - Tukey pairwise comparisons

RSSI ANALYSIS			
Tag Carrying Position	N	Mean	Grouping
13	10	-44,30	A
12	10	-57,60	B
14	10	-59,90	BC
2	10	-66,90	CD
1	10	-67,90	CD
7	10	-68,10	D
3	10	-68,50	D
10	10	-68,90	DE
11	10	-70,10	DE
5	10	-76,80	EF
8	10	-79,60	F
9	10	-90,00	G
6	10	-92,00	G
4	10	-92,00	G

Source: Prepared by the author, 2019.

To prove these results, the two tags were then evaluated in a controlled environment. Using the Center for Research and Development in Telecommunications (CPqD) laboratory, Figure 53, it was swept frequency range of 860-915 MHz and evaluated the received power

needed to recognize the tags "c" (Figure 54a) and "d" (Figure 54b). As shown in Figure 54, the

tag "d" has a better reading sensitivity within the entire UHF spectrum.

Figure 53 - Using the CPqD laboratory to evaluate the prototype tag
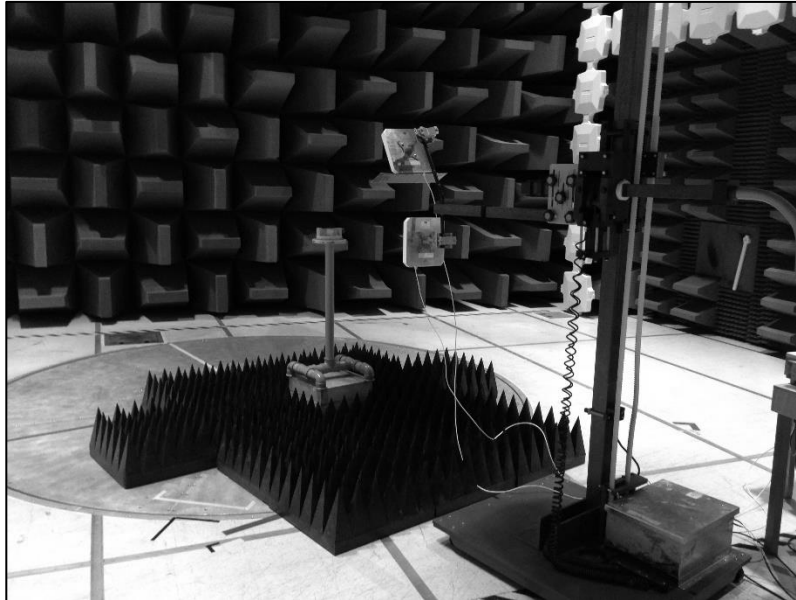
Source: Prepared by the author, 2019.

Figure 54 - Power received by the reader antenna for tag recognition
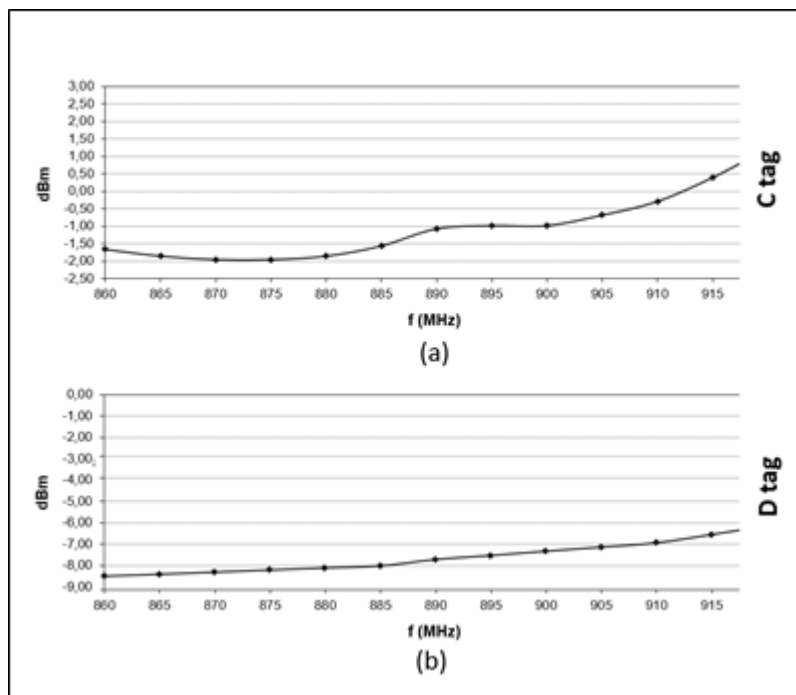
Source: Prepared by the author, 2019.

After finding the tag that has the best recognition performance, in other words, the tag that requires a lower reception power of the reader antennas for the correct interpretation, was analyzed the power required to recognize the tag according the positions 3, 7 and 9 shown in Table 3. As shown in Figure 55, the tag's sensitivity level is dependent on the carrying position. The Figure 55a shows the tag response when positioned horizontally in contact with the mobile phone is very poor, requiring 9 dBm for recognition at 890 MHz. The Figure 55b represents the same scene, but with the tag positioned vertically. The recognition in this case is even worse, requiring 10 dBm at the same frequency. The Figure 55c is the tag in the hand of a volunteer, but being carried with part of the card exposed. This form of carrying position facilitates more reading as can be seen in the graph, because the power required for tag recognition is lower, very different from the result shows in Figure 55d which the tag is totally hidden by hand. Finally, the Figure 55e shows the results when the tag is in the front pocket of the volunteer's pants, Figure 56. This is the best performance of the four forms of position evaluated, as it demands the lowest reading power for tag recognition.

Figure 55 - Tag sensitivity test according the power received by the reader antenna (with some position from Table 3)
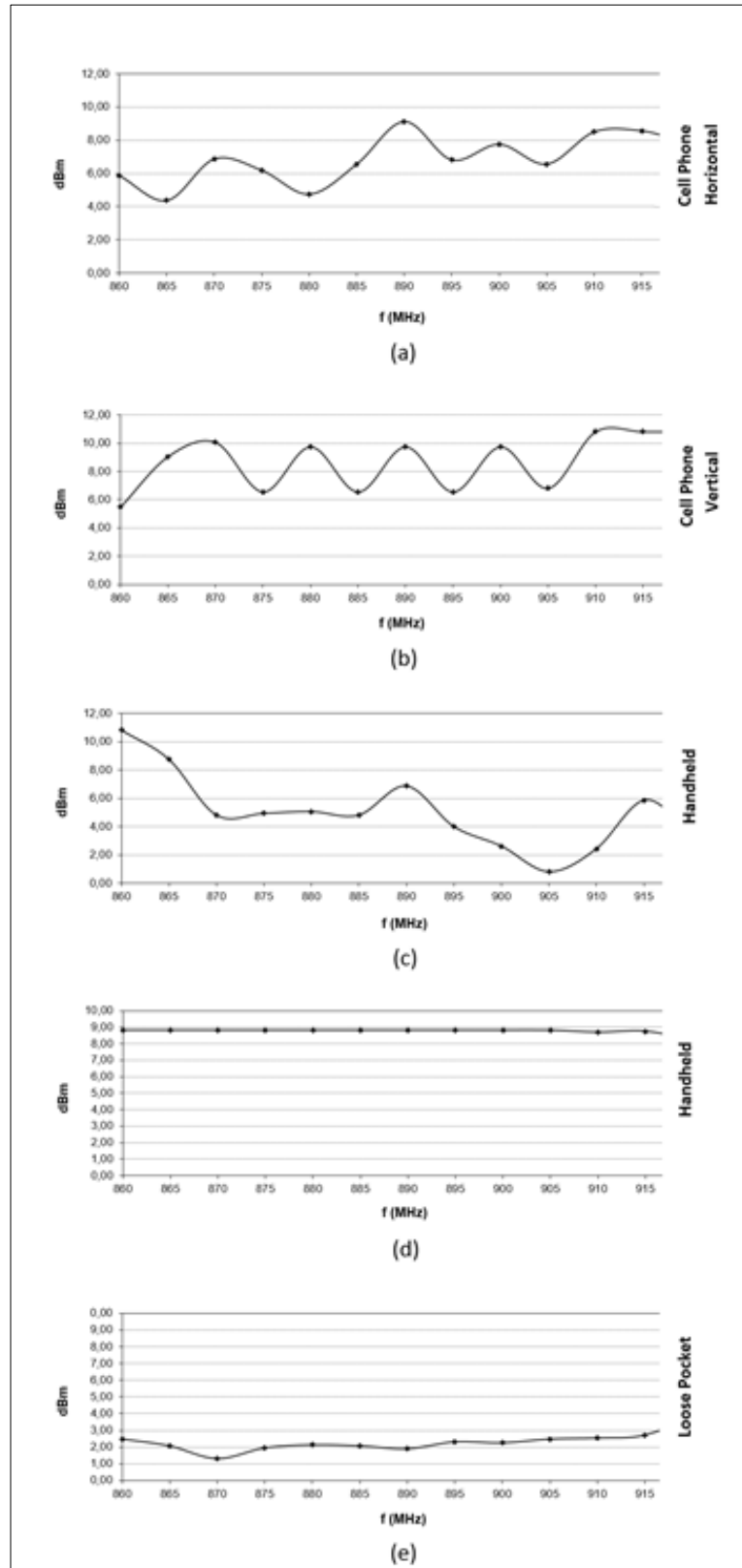
Source: Prepared by the author, 2019.

Figure 56 - In the front pocket of pants

Source: Prepared by the author, 2019.

The third and final phase of the test was the collective assessment of users. Ten volunteers from different biotypes crossed the portal five times carrying the tags in the 14 positions shown in Table 3. All used cards containing the tag "d". The ratio of weight, height and BMI for each volunteer are reported in Table 14.

Table 14 - Volunteers data

Volunteer	Height	Weight	BMI
1	179 cm	70 kg	21.8
2	175 cm	66 kg	21.5
3	187 cm	92 kg	26.3
4	170 cm	85 kg	29.4
5	179 cm	79 kg	24.6
6	180 cm	92 kg	28.3
7	176 cm	75 kg	24.2
8	183 cm	85 kg	25.3
9	180 cm	80 kg	24.6
10	170 cm	65 kg	22.4

Source: Prepared by the author, 2019.

The Table 15 presents the RSSI values obtained by the volunteer with the bigger recognition number (volunteer 1) and with the fewer recognition number (volunteer 9). As higher the RSSI, the stronger the received signal, therefore values equal to -92 or lower represent non-recognition of the tag.

Based on the recognition information obtained in the collective test, it was possible to make a comparison to the data obtained in the first phase of the study, Table 16.

Finally, the volunteers passed through the portal in pairs to evaluate the effectiveness of the system when more than one user is crossing the reading antennas. Each pair used a carrying position of the tag and crossed by the portal five times as shown in Table 17.

Table 15 - RSSI analysis with volunteer 1 and volunteer 9

RSSI ANALYSIS										
Ref.	Volunteer 1					Volunteer 9				
Table 3	S1	S2	S3	S4	S5	S1	S2	S3	S4	S5
1	-62	-62	-57	-55	-57	-66	-65	-66	-92	-64
2	-62	-56	-70	-62	-61	-56	-64	-92	-64	-62
3	-68	-66	-66	-66	-92	-62	-61	-51	-51	-62
4	-69	-92	-92	-92	-92	-92	-92	-92	-92	-69
5	-70	-69	-70	-68	-70	-64	-62	-58	-59	-66
6	-92	-92	-92	-92	-92	-92	-92	-92	-92	-92
7	-61	-60	-45	-70	-63	-56	-58	-92	-64	-57
8	-54	-62	-62	-68	-63	-92	-92	-61	-54	-92
9	-92	-92	-53	-92	-92	-65	-92	-55	-92	-92
10	-53	-63	-55	-56	-64	-62	-62	-62	-62	-67
11	-62	-58	-62	-57	-63	-65	-59	-55	-64	-63
12	-53	-57	-59	-62	-57	-55	-92	-58	-92	-52
13	-70	-70	-69	-66	-70	-70	-67	-69	-71	-66
14	-55	-56	-62	-53	-56	-57	-92	-92	-68	-71

> -92 = Recognized card

≤ -92 = Unrecognized card

Source: Prepared by the author, 2019.

Table 16 - Recognition analysis between collective and two volunteers

	RECOGNITION ANALYSIS			
Ref.	P2 (Collective)		P1 (Two Volunteers)	
Table 3	Recognition	%	Recognition	%
1	49	98	10	100
2	44	88	10	100
3	43	86	10	100
4	7	14	0	0
5	42	84	9	90
6	2	4	0	0
7	48	96	10	100
8	38	76	10	100
9	9	18	4	40
10	50	100	10	100
11	50	100	10	100
12	38	76	10	100
13	50	100	10	100
14	45	90	10	100

Source: Prepared by the author, 2019.

Table 17 - Results in volunteers passing in pair through the portal

	DOUBLE ROW ANALYSIS									
Ref.	Volunteer 2					Volunteer 7				
Table 3	S1	S2	S3	S4	S5	S6	S7	S8	S9	S10
1	X	X	X	X	X	X	X	X	0	X
	Volunteer 3					Volunteer 8				
2	X	X	X	X	X	0	X	X	0	X
	Volunteer 4					Volunteer 9				
11	X	X	X	X	X	X	X	X	X	0
	Volunteer 5					Volunteer 10				
12	X	X	X	X	X	X	X	X	X	X
	Volunteer 1					Volunteer 6				
14	X	X	X	X	X	X	X	X	X	X

X – Recognized card

0 – Unrecognized card

Source: Prepared by the author, 2019.

8 DISCUSSION

According to the presented results, it was possible to evaluate first the system performance for two volunteers. In the first test, with the choice of the best tag within a group of four options, there was recognition of 81.42% of volunteer A against 60% of volunteer B, considering the heights of the antennas presented by (OBERLI, 2010). This wide variation is directly linked to the height of the volunteers, because the reading antennas are directional, restricting the reading region. Further analysis with the set of antennas 1 and 3 to 100 cm and antennas 2 and 4 to 78 cm was enough to have closer results. In this configuration, for the volunteer A it showed 78.57% of recognition success and for the volunteer B, 77.14%. An important aspect to be noticed is the fact that the volunteer A, with higher BMI, had always shown results with higher recognition compared to volunteer B, which has lower BMI. The response may be in the form of the tag carrying position. Since the volunteer A is higher, the tags tend to be better positioned in relation to the side antennas, facilitating their reading.

The results of the performance tests done in a controlled environment made possible to understand how the reading can be influenced by the tag carrying position. Even using the most efficient tag in the general context of the tests with two volunteers, it was revealed different responses depending on the form of tag carrying. In the collective test, where standardization in the tag carrying way is more difficult to maintain, the recognition range was 80% to 68.57% within ten volunteers group.

The tests have shown that some forms of tag carrying are difficult to recognize. The tests with the tag on socks and in a pocket with a cell phone showed very low performance. The tag carried on socks practically forces the application of antennas about 20 cm from the ground. The cell phone generates strong influence on the tag due to its operation in a wide range of RF

networks (Wi-Fi, Global System for Mobile Communications (GSM), Bluetooth, etc.), that generates interference in tag reading.

Excluding the results obtained with the carrying positions 4, 6 and 9 (Table 3), the recognition range considering the tests with two volunteers was 94.54% to 100% and with the collective test was 81.81% to 98.18%.

According to the conducted research that raised the 14 tag carrying positions, the most favorable region for carrying the card is the region of the waist. From the 14 possible user carrying positions tested here, 11 were in the waist area. Thus, the system has proven most effective when set to 100 cm and 78 cm from the ground. The positions with high recognition have references 1, 2, 3, 5, 7, 10, 11 and 13 (Table 3).

This experiment, elaborated to determine if the volunteer and the tag carrying position are related with the RSSI level, proved that in fact, only the tag carrying position is really significant in this situation. Anyway, the interaction between the volunteer and the tag carrying position also interferes at the RSSI level.

Until now the expectations are great to get good results with this technique proposed to passenger detection, but it is necessary to go further with the work.

The two controllable factors idealized seem to suffice to have an idea of the functionality of the proposed system, but may not guarantee a high level of reliability, so it may be necessary to analyze other factors. Another important aspect to be evaluated is the repetitiveness of the experiment. Five evaluations with each volunteer per tag carrying type may also not be sufficient to obtain a good statistical basis, although the power test proved to be adequate.

In terms of the cost of the solution, it is important to note that the antennas and reader used are solutions already consolidated in the market for other applications, that is, they may not be the best options considering the recognition of passengers in public transport vehicles.

In this sense it is necessary to develop antennas and UHF RFID reader dedicated to the application to make the solution viable commercially.

9 CONCLUSION

Finding a way to count passengers that use public transport cheaply and effectively is still an incessant search of the market, but there are technologies that can be directed to this application in order to solve or minimize the existing problems. One of the ways that is interesting and feasible was presented in this work.

The possibility of not only counting passengers but also recognizing them is something that has not been explored in the scientific world. As discussed in this thesis the focus of today's solutions is not to recognize individual passengers, but if a technological solution allows this, open a new range of possibilities in the context of smart cities. Being able to know exactly what public transport means, when and where each citizen goes, are data that can contribute to a broader schematization of services.

The proposed passenger recognition system for public transport via UHF card is still a process to be improved, but presents results that motivate the continuation of the studies. The work so far directed to this area was confined to a few forms of tag carrying positions, which led to preliminary conclusions. The work presented in this thesis shows, in a setting of 14 carrying positions, which suitably positioned reading antennas and the use of tags designed exclusively for this application have the recognition rate of over to 80%. The level below the initial expectation owes much to some forms of tag carrying positions raised in the research with public transport users. For example, carrying the card on socks and along with the cell phone are attitudes that hinder the recognition of the tag by the system. On the other hand, more conventional forms of carrying, as in the pockets of pants or shirts, showed extremely high levels of recognition.

The improvement of the system configuration exposed in this thesis can contribute to new works focusing this line of research. Additional experiments can be performed in order to find ways to hinder the detected problems related to carrying positions and scenarios.

Automation and especially interactivity of systems without the need of user actions enables the creation of a wider network of geo-location, contributing to a more effective and intelligent public transport system. In a current scenario, for example, it would be possible at first to automatically determine which vehicle models should be used at certain times during the day, all according to a historical basis of use, generated through the recognition of passengers, registering when he got in and out of the vehicle and where each event occurred. This will be the next step of this work, to gather the study of passenger recognition with the use of geolocation and data sent to the cloud to, through a relationship and planning algorithm, manage the public transport fleet in order to have a service of quality, with rational use of the resources and attendance of the population.

REFERENCES

ACURA. 100.098: Antena UHF Mono-Estática. Acura Global. [S. l.]. 1 p. Available in: <http://www.acura.com.br/pt/produtos/antena?task=callelement&format=raw&item_id=203&element=4b68739a-1a2d-4743-b3eb-7bddb8f63bfd&method=download> Access in: 17 Mar. 2016.

AHSON, S.; ILYAS, M. **RFID Handbook: Applications, Technology, Security, and Privacy.** Boca Raton, FL: Taylor & Francis Group, 2008. 712 p. ISBN-13: 978-1-4200-5499-6

ALBUQUERQUE, C. Qualiônibus: Pesquisa de Satisfação. EMBARQ Brasil, [S. l.], 2014. 40 p. Available in: <http://wricidades.org/node/47381>. Access in: 10 Sep. 2017.

BALANIS, C. A. **Antenna Theory: Analysis and Design.** Hoboken, NJ: John Wiley & Sons, 2005. 1136 p. ISBN: 0-471-66782-X

BOX, G. E. P.; HUNTER, J. S.; HUNTER, W. G. **Statistics for Experimenters: Design, Innovation, and Discovery.** Hoboken, NJ: John Wiley & Sons, 2005. 633 p. ISBN-13: 978-0471-71813-0

BRAGA, M. L. et al. Anytime route planning with constrained devices. **Computers & Electrical Engineering**, [S. l.], v. 54, p. 53-67, Aug. 2016. Available in: <https://doi.org/10.1016/j.compeleceng.2016.07.011>. Access in: 8 Sep. 2017.

CHEN, J. et al. Automatic Head Detection for Passenger Flow Analysis in Bus Surveillance Videos. In: 2012 5TH INTERNATIONAL CONGRESS ON IMAGE AND SIGNAL PROCESSING, 5, 2012, **Proceedings . . .** Chongqing, China, 2012. p. 143-147. Available in: <https://doi.org/10.1109/CISP.2012.6469669>. Access in: 5 Nov. 2017.

CHENG, Y.; CHEN, S. Adoption forecasting of multipurpose smart cards in transit systems. **Journal of Intelligent Transportation Systems**, [S. l.], v. 20, p. 363-384, May 2016. Available in: <http://doi.org/10.1080/15472450.2016.1191993>. Access in: 8 Sep. 2017.

CST. CST MICROWAVE STUDIO: Workflow & Solver Overview, Ver. 2010. CST - Computer Simulation Technology AG. [S. l.], 2010. 110 p. 1 CD-ROM.

DENNISON, A. AD-370u7 NEL: UHF RFID Inlays. Avery Dennison Corp. Miamisburg, OH, 2018. 1 p. Available in: <https://rfid.averydennison.com/content/dam/averydennison/rfid/Global/documents/datasheets/AD-370u7-NEL-Datasheet-v1.pdf> Access in: 10 Feb. 2018.

DOBKIN, D. M. **The RF in RFID: UHF RFID in Practice.** Waltham, MA: Elsevier Inc., 2013. 540 p. ISBN-13: 978-0-12-394583-9

FIORI, A.; MIGNONE, A.; ROSPO, G. DeCoClu: Density consensus clustering approach for public transport data. **Information Sciences**, [S. l.], v. 328, p. 378-388, Jan. 2016. Available in: <https://doi.org/10.1016/j.ins.2015.08.054>. Access in: 8 Sep. 2017.

GAL, A. et al. Traveling time prediction in scheduled transportation with journey segments. **Information Systems**, [S. l.], v. 64, p. 266-280, Mar. 2017. Available in: <https://doi.org/10.1016/j.is.2015.12.001>. Access in: 9 Sep. 2017.

GHASEMZADEH, M. et al. Anonymizing trajectory data for passenger flow analysis. **Transportation Research Part C: Emerging Technologies**, [S. l.], v. 39, p. 63-79, Feb. 2014. Available in: <https://doi.org/10.1016/j.trc.2013.12.003>. Access in: 8 Sep. 2017.

GLOVER, B.; BHATT, H. **RFID Essentials.** Sebastopol, CA: O'Reilly Media, 2006. 278 p. ISBN: 0-596-00944-5

GOES, A. A. **Modelo de Propagação Empírico para Sistemas RFID Passivo.** 2014. 79 p. Tese (Doutorado em Engenharia Elétrica) – Programa de Pós-Graduação em Engenharia Elétrica, Universidade Estadual de Campinas, Campinas, 2014.

GREFF, P. A. **Especificação de um Sistema para Monitoramento de Atividades de Natação usando RFID.** 2009. 81 p. Monografia (Tecnólogo em Sistemas de Telecomunicações) – Curso Superior de Tecnologia em Sistemas de Telecomunicações, Instituto Federal de Educação, Ciência e Tecnologia de Santa Catarina, São José, 2009.

HECKEL, A. P. **Identificação por Radiofrequência (RFID) Estudo Teórico e Experimentação via Simulação.** 2007. 102 p. Monografia (Bacharelado em Ciência da Computação) – Instituto de Ciências Exatas e Tecnológicas, Universidade Feevale, Novo Hamburgo, 2007.

HILDÉN, E.; OJALA, J.; VÄÄNÄNEN, K. User Needs and Expectations for Future Traveling Services in Buses. In: NORDIC CONFERENCE ON HUMAN-COMPUTER INTERATION, 9, 2016, **Proceedings . . .** Gothenburg, Sweden, 2016. 6 p. ISBN: 978-1-4503-4763-1 Available in: <https://doi.org/10.1145/2971485.2996733>. Access in: 10 Sep. 2017.

HU, X.; ZHAO, L.; WANG, W. Impact of perceptions of bus service performance on mode choice preference. **Advances in Mechanical Engineering**, [S. l.], v. 7, p. 1-11, Apr. 2015. Available in: <https://doi.org/10.1177/1687814015573826>. Access in: 9 Sep. 2017.

MALISON, P.; PROMWONG, S.; SUKUTAMATANTI, N. Characterization of Double Directional RFID in an Indoor Environment with Human Body. In: INTERNATIONAL CONFERENCE ON COMPUTER AND COMMUNICATION ENGINEERING, 2008, **Proceedings . . .** Kuala Lumpur, Malaysia, 2008. p. 1027-1031. Available in: <https://doi.org/10.1109/ICCCE.2008.4580764>. Access in: 27 Mar. 2016.

MONTGOMERY, D. C. **Design and Analysis of Experiments.** Hoboken, NJ: John Wiley & Sons, 2012. 730 p. ISBN-13: 978-1-118-14692-7

MONTHLY. Popular Science, v. 102, n. 4. Bonnier Corporation, New York, 1923. p. 59. Available in: <https://books.google.com.br/books?id=VCoDAAAAMBAJ&lpg=PA1&dq=Popular%20Science%20vol.%20102&hl=pt-BR&pg=PA1#v=onepage&q=Popular%20Science%20vol.%20102&f=false>. Access in: 2 Oct. 2018.

MORENO, G. N. M. **Avaliação e Aplicação da Tecnologia RFID na Gestão da Cadeia do Frio de Frutas.** 2016. 188 p. Dissertação (Mestrado em Engenharia Mecânica) – Programa de Pós-Graduação em Engenharia Mecânica, Universidade Estadual de Campinas, Campinas, 2016.

NUNES, A. A.; DIAS, T. G.; CUNHA, J. F. Passenger Journey Destination Estimation From Automated Fare Collection System Data Using Spatial Validation. **IEEE Transactions on Intelligent Transportation Systems**, [S. l.], v. 17, p. 133-142, Jan. 2016. Available in: <https://doi.org/10.1109/TITS.2015.2464335>. Access in: 27 Sep. 2017.

NXP. SL3S1204: UCODE 7 data sheet, Rev. 3.9. NXP B. V. [S. l.], Mar. 2017. 40 p. Available in: <https://www.nxp.com/docs/en/data-sheet/SL3S1204.pdf>. Access in: 15 Oct. 2017.

OBERLI, C.; TORRITI, M. T.; LANDAU, D. Performance Evaluation of UHF RFID Technologies for Real-Time Passenger Recognition in Intelligent Public Transportation Systems. **IEEE Transactions on Intelligent Transportation Systems**, [S. l.], v. 11, p. 748-753, Sep. 2010. Available in: <https://doi.org/10.1109/TITS.2010.2048429>. Access in: 28 Apr. 2016.

OLIVEIRA, A. S.; PEREIRA, M. F. **Estudo da tecnologia de identificação por radiofrequência - RFID.** 2006. 85 p. Monografia (Bacharelado em Engenharia Elétrica) – Departamento de Engenharia Elétrica, Universidade de Brasília, Brasília, 2006.

PINNA, I.; CHIARA, B. D.; DEFLORIO, F. P. Automatic Passenger Counting Systems for Public Transport. **Intelligent Transport**, [S. l.], n. 6, Dec. 2010. Available in: <https://www.intelligenttransport.com/transport-articles/3116/automatic-passenger-counting-systems-for-public-transport/>. Access in: 2 Oct. 2018.

ROEHRIG, R. **Um estudo sobre a viabilidade de implantação de etiquetas inteligentes como vantagem competitiva em um Centro de Distribuição.** 2005. 85 p. Monografia (MBA em Gerência de Sistemas Logísticos) – Centro de Pesquisa e Pós-Graduação em Administração, Universidade Federal do Paraná, Curitiba, 2005.

SANTINI, A. G. **RFID: Radio Frequency Identification.** Rio de Janeiro, RJ: Ciência Moderna, 2008. 96 p. ISBN: 978-8-573-93716-9

SENNOU, A. S. et al. An Interactive RFID-based Bracelet for Airport Luggage Tracking System. In: INTERNATIONAL CONFERENCE ON INTELLIGENT SYSTEMS, MODELING AND SIMULATION, 4, 2013, **Proceedings . . .** Bangkok, Thailand, 2013. p. 40-44. Available in: <https://doi.org/10.1109/ISMS.2013.29>. Access in: 13 May 2016.

SIRIT. RSI-650 Inlay: 865-928 MHz Global, Passive Transponder. Sirit Inc. [S. l.]. 1 p. Available in: <http://upway.pl/images/produkty/specyfikacje_tagow_rfid/tag_rfid_specyfikacj a_04.pdf> Access in: 22 Apr. 2016.

SIRIT. RSI-654 Inlay: 865-928 MHz Global, Passive Transponder. Sirit Inc. [S. l.]. 1 p. Available in: <http://www.upway.pl/images/produkty/specyfikacje_tagow_rfid/tag_rfid_specy fikacja_05.pdf> Access in: 22 Apr. 2016.

TASHI; HASAN, M. S.; YU, H. Design and Simulation of UHF RFID Tag Antennas and Performance Evaluation in Presence of a Metallic Surface. In: INTERNATIONAL

CONFERENCE ON SOFTWARE, KNOWLEDGE INFORMATION, INDUSTRIAL MANAGEMENT AND APPLICATIONS (SKIMA) PROCEEDINGS, 5, 2011, **Proceedings . . .** Benevento, Italy, 2011. 5 p. Available in: <https://doi.org/10.1109/SKIMA.2011.6089974>. Access in: 10 May 2016.

THINGMAGIC. Mercure6e: M6e Hardware Guide, Firmware Ver. 1.13.1 and later. ThingMagic, a division of Trimble Navigation Limited. Cambridge, MA, 2013. 100 p. 1 CD-ROM.

TSAI, M. et al. UHF RFID PIFA Array Tag Antenna for Human Body Applications. In: INTERNATIONAL SYMPOSIUM ON WIRELESS PERSONAL MULTIMEDIA COMMUNICATIONS, 15, 2012, **Proceedings . . .** Taipei, Taiwan, 2012. p. 434-437. Available in: <https://ieeexplore.ieee.org/document/6398749>. Access in: 10 May 2016.

ZHANG, F. et al. On Geocasting over Urban Bus-Based Networks by Mining Trajectories. **IEEE Transactions on Intelligent Transportation Systems**, [S. l.], v. 17, p. 1734-1747, Jun. 2016. Available in: <https://doi.org/10.1109/TITS.2015.2504513>. Access in: 27 Sep. 2017.

ZÖSCHER, L. et al. Concept for a Security Aware Automatic Fare Collection System Using HF/UHF Dual Band RFID Transponders. In: EUROPEAN SOLID STATE DEVICE RESEARCH CONFERENCE (ESSDERC), 45, 2015, **Proceedings . . .** Graz, Austria, 2015. p. 194-197. Available in: <https://doi.org/10.1109/ESSDERC.2015.7324748>. Access in: 28 Oct. 2017.